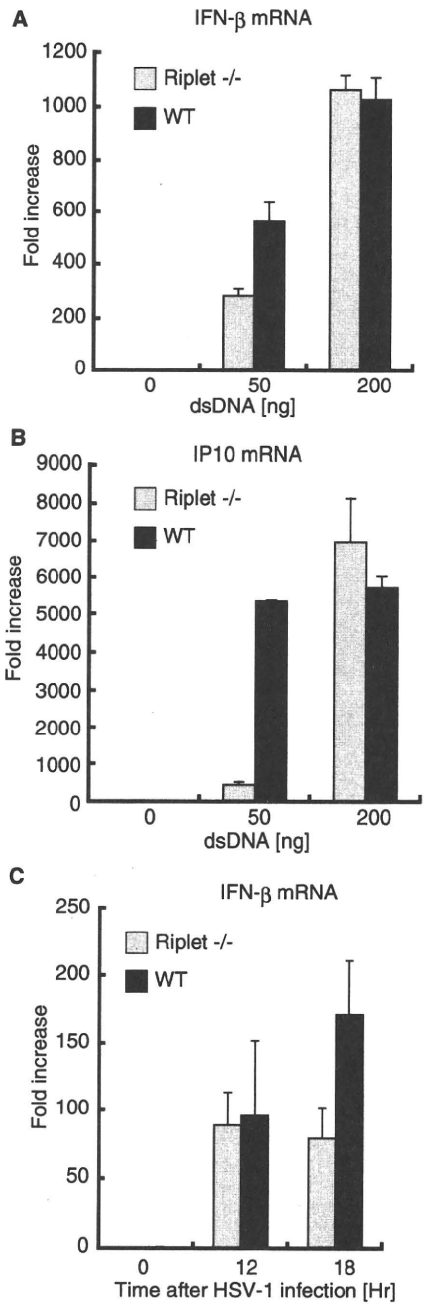

Figure 4. Role of Riplet in Type I IFN Production Induced by Cytoplasmic dsDNA

(A and B) Wild-type and *Riplet*$^{-/-}$ MEFs were transfected with the indicated amounts of dsDNA (Salomon sperm DNA) using the Lipofectamine 2000 reagent. Nine hours after the transfection, IFN-β (A) and IP-10 (B) mRNA expression was determined by RT-qPCR. Data are shown as means ±SD and are representative of three independent experiments.

(C) Wild-type and *Riplet*$^{-/-}$ MEFs were infected with HSV-1 at moi = 4, and IFN-β mRNA expression at the indicated times was examined by RT-qPCR. Data are shown as means ±SD and are representative of three independent experiments.

6A–6F). Similar to cDCs, cytokine production was reduced in Riplet knockout mice (Figures 6A–6F). Peritoneal Mf were isolated from wild-type and *Riplet*$^{-/-}$ mice. Knockout of Riplet reduced type I IFN production from peritoneal Mfs during VSV infection (Figures S4C and S4D).

We next generated Flt3L-induced DCs (Flt3L-DCs), which contain pDCs. Akira and his colleagues previously showed that the knockout of RIG-I or IPS-1 does not reduce type I IFN and IL-6 production by Flt3L-DCs, because RIG-I is dispensable for cytokine production in pDCs (Kato et al., 2005). The Flt3L-DCs of *Riplet*$^{-/-}$ mice produced normal amounts of IFN-a, -β, and IL-6 during Flu infection (Figures 6A–6F). This is consistent with the notion that Riplet is essential for the RIG-I-mediated type I IFNs and IL-6 production. Although the IFN-α levels in the culture medium after VSV infection were comparable with those in wild-type and *Riplet*$^{-/-}$ mice, Flt3L-DCs of *Riplet*$^{-/-}$ mice produced less IL-6 compared with that produced by wild-type mice through an unknown mechanism (Figure 6C).

Next, we examined type I IFN production during SeV infection. SeV infection induced IFN-α and -β productions from wild-type BM-DC, and the knockout of Riplet reduced IFN-α and -β productions from BM-DC (Figures S4E–S4J). Wild-type Flt3L-DC produced IFN-α after SeV infection, and the knockout of Riplet did not reduce IFN- α production from Flt3L-DC (Figures S4E–S4J).

Riplet Is Essential for Antiviral Immune Defense In Vivo

To investigate the role of Riplet in antiviral responses in vivo, wild-type and *Riplet*$^{-/-}$ mice were injected intraperitoneally with wild-type VSV, and sera were collected to measure type I IFN and IL-6 levels. IFN-α, -β, and IL-6 levels in sera were markedly reduced in *Riplet*$^{-/-}$ mice compared to in wild-type mice (Figures 7A and 7B, and Figure S5A). Next, wild-type and *Riplet*$^{-/-}$ mice were intranasally infected with VSV, and type I IFN levels in their sera were measured. At early time points, IFN-α and -β production was reduced in *Riplet*$^{-/-}$ mice compared to wild-type mice (Figures 7C and 7D); however, cytokine levels were comparable at later time points (Figures S5B and S5C). Previously, Ishikawa et al. observed that the knockout of STING gene, which is involved in RIG-I-dependent signaling, leads to reduction of type I IFN at early time points and relatively less reduction at later time points (Ishikawa and Barber, 2008; Ishikawa et al., 2009).

To determine if Riplet deficiency affects the survival of mice after VSV infection, the mice were intranasally infected with VSV, and their survival was monitored. Wild-type mice survived VSV infection; however, *Riplet*$^{-/-}$ mice were susceptible to VSV infection (Figure 7E). The viral titer in *Riplet*$^{-/-}$ mice brains 7 days after infection was higher than in wild-type mice (Figure 7F). These data indicate that Riplet plays a key role in the host defenses against VSV infection in vivo, and type I IFN production at early time points is important for host defenses.

DISCUSSION

In this study, we presented genetic evidence that Riplet is indispensable for antiviral responses in MEFs, BM-Mf, and BM-DCs, but not in Flt3L-DCs. The cell-type-specific requirement of Riplet

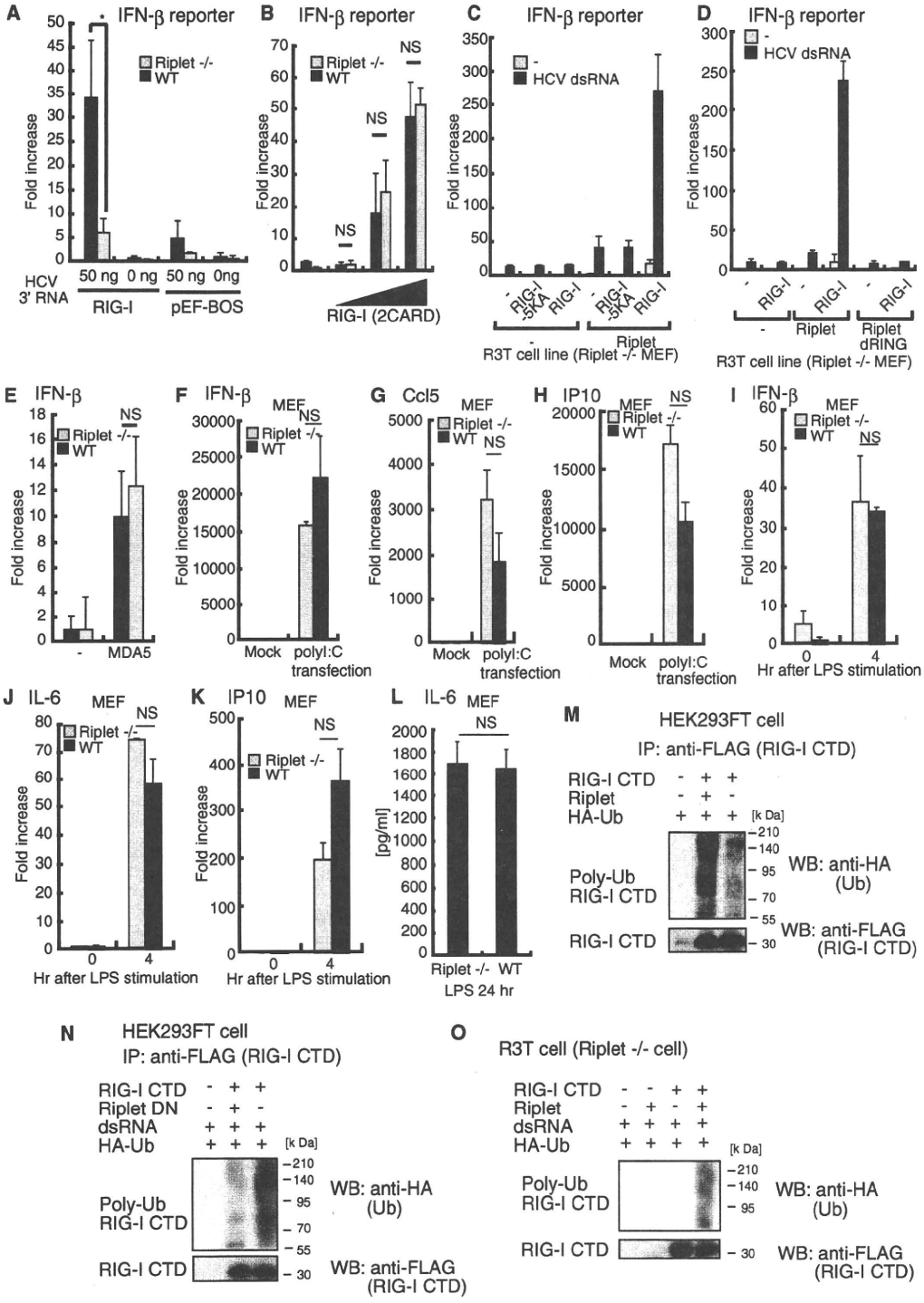

Figure 5. Role of Riplet in the RIG-I-Dependent Pathway

(A) Expression vector of full-length RIG-I and reporter plasmids were transfected into wild-type or *Riplet*$^{-/-}$ MEFs with or without HCV 3′UTR short dsRNA, and after 24 hr IFN-β promoter activation was examined by reporter gene assay. Data are shown as means ±SD and are representative of three independent experiments. *$p < 0.05$ (t test).

is similar to that of RIG-I. Previously, we showed that Riplet binds to RIG-I and mediates Lys63-linked polyubiquitination of RIG-I (Oshiumi et al., 2009). Genetic evidence in this study revealed that Riplet function is essential for RIG-I-dependent type I IFN production. Knockout of Riplet reduced type I IFN production in vivo during the early phase of VSV infection, and *Riplet*$^{-/-}$ mice were susceptible to VSV infection. Taken together, our results provide genetic evidence that Riplet is essential for RIG-I-dependent antiviral immune response in vivo. Most *RIG-I*$^{-/-}$ embryos were lethal at embryonic days 12.5–14.0 in some strain backgrounds (Kato et al., 2005). However, we could not observe any developmental defect in Riplet knockout mice as far as we examined.

Previously, Chen and his colleagues independently isolated Riplet and named it REUL (Gao et al., 2009). They reported that REUL/Riplet binds to RIG-I CARDs but not to CTD (Gao et al., 2009). Furthermore, they reported that REUL/Riplet mediates Lys63-linked polyubiquitination of Lys172 of RIG-I CARDs in a manner similar to TRIM25 (Gack et al., 2007; Gao et al., 2009). Although they did not show any expression profile data for Riplet and TRIM25, they mentioned that TRIM25 and Riplet have different distribution patterns, and thus hypothesized that REUL/Riplet is a complementary factor of TRIM25 and is required for RIG-I activation in cells that do not express TRIM25 (Gao et al., 2009). However, our genetic evidence is not consistent with their hypothesis, because Riplet is essential for RIG-I activation in MEFs that express TRIM25. Previously, Gack et al. showed that knockout of TRIM25 alone abolished RIG-I activation in MEFs (Gack et al., 2007). Therefore, null mutation in either Riplet or TRIM25 abolishes RIG-I activation. This genetic evidence indicates that Riplet can mediate polyubiquitination of RIG-I Lys residues that are not ubiquitinated by TRIM25. This means that Riplet functions differently than TRIM25 in RIG-I activation.

We isolated Riplet cDNA by yeast two-hybrid screening using the C-terminal region of RIG-I (Oshiumi et al., 2009). Because the yeast genome does not encode RIG-I, the interaction indicates the direct binding of Riplet to the RIG-I C-terminal region. The interaction between RIG-I CTD and Riplet has also been confirmed by immunoprecipitation assays in human cells (Oshiumi et al., 2009). Moreover, we have shown that Riplet expression leads to Lys63-linked polyubiquitination of RIG-I CTD (Oshiumi et al., 2009). Recently, Zheng et al. showed that RIG-I CARDs has the ability to bind to polyubiquitin chains (Zeng et al., 2010). We have carefully detected Riplet-mediated polyubiquitination of RIG-I C-terminal region without CARDs, under high-salt conditions, in which many protein-protein interactions were abolished (Oshiumi et al., 2009). Therefore, we proposed the hypothesis that Riplet mediates Lys63-linked polyubiquitination of RIG-I CTD (Oshiumi et al., 2009). This model can explain the genetic evidence that Riplet is essential for RIG-I activation in MEFs that express TRIM25. Gack et al. showed that K172R mutation alone caused near-complete loss of ubiquitination of the human RIG-I CARDs (Gack et al., 2007). Because residue 172 of mouse RIG-I is not Lys but Gln (Shigemoto et al., 2009), Riplet/Reul does not ubiquitinate residue 172 of mouse RIG-I. Based on the previous studies and our current data, we prefer the interpretation that Riplet activates RIG-I through polyubiquitination of RIG-I CTD. However, this interpretation does not exclude the possibility that Riplet ubiquitinates both CTD and CARDs of RIG-I (Gao et al., 2009; Oshiumi et al., 2009).

Previously, we showed that Lys849, -851, -888, -907, and -909 are critical residues in Riplet-mediated RIG-I CTD ubiquitination (Oshiumi et al., 2009). These five Lys residuse are close to the dsRNA binding sites of RIG-I CTD (Takahasi et al., 2008), and the 5KA mutation weakly reduced RNA binding activity of RIG-I. Therefore, it is possible that the 5KA mutation abrogate activation and polyubiquitination of RIG-I by reducing RNA biding activity of RIG-I. However, this possibility is weakened by following observations. First, the 5KA mutation caused near-complete loss of RIG-I activation, but the RIG-I-5KA mutant protein still possessed RNA binding activity. Second, overexpression of Riplet led to RIG-I activation in the absence of dsRNA in HEK293 cells, and this ligand-independent activation of RIG-I

(B) Expression vector for the two RIG-I N-terminal CARDs were transfected into wild-type or *Riplet*$^{-/-}$ MEFs together with reporter plasmids, and IFN-β promoter activation was examined by the reporter gene assay. Data are shown as means ±SD and are representative of three independent experiments. "NS" indicates not statistically significant.

(C) Empty, wild-type RIG-I-, or RIG-I-5KA mutant-expressing vectors were transfected into the *Riplet*$^{-/-}$ MEF cell line together with or without the Riplet-expressing vector. Cells were stimulated with HCV 3′UTR short dsRNA, and reporter gene assay was performed as described in (A).

(D) Empty or wild-type RIG-I-expressing vectors were transfected into the *Riplet*$^{-/-}$ MEF cell line together with empty, wild-type Riplet, or Riplet mutant (Riplet dRING)-expressing vector. Cells were stimulated with HCV 3′UTR short dsRNA, and the reporter gene assay was performed as described in (A).

(E) Empty or MDA5-expressing vectors was transfected into wild-type or *Riplet*$^{-/-}$ MEFs together with reporter plasmids, and after 24 hr IFN-β promoter activation was examined by the reporter gene assay.

(F–H) Of poly(I:C), 0.8 μg was transfected into wild-type or *Riplet*$^{-/-}$ MEFs. Twenty-four hours after transfection, total RNA was extracted from MEFs and subjected to RT-qPCR to determine IFN-β (F), Ccl5 (G), and IP10 (H) expression. Expression in each sample was normalized to the β-actin mRNA expression.

(I–K) Wild-type or *Riplet*$^{-/-}$ MEFs were stimulated with 1 μg of LPS. Total RNA was extracted at the indicated times and subjected to RT-qPCR analysis for of IFN-β (I), IL-6 (J), or IP-10 (K) expression.

(L) Wild-type or *Riplet*$^{-/-}$ MEFs were stimulated with LPS, and after 24 hr the amount of IL-6 in culture supernatants was measured by ELISA.

(M) HEK293FT cells were transfected with Riplet, FLAG-tagged RIG-I-CTD, and HA-tagged ubiquitin (HA-Ub) expression vectors. Twenty-four hours after transfection, cell lysates were extracted and immunoprecipitation was carried out with anti-FLAG antibody as previously described (Oshiumi et al., 2009). The samples were analyzed by SDS-PAGE, and western blotting was performed using anti-HA polyclonal antibody (Ub) and anit-Flag M2 monoclonal antibody (RIG-I-CTD). The plasmids are described previously (Oshiumi et al., 2009).

(N) Expression vector of dominant negative form of Riplet (Riplet DN) was transfected into HEK293FT cells together with expression vector of FLAG-tagged RIG-I CTD and HA-tagged ubiquitin. Cells were stimulated with dsRNA. Ubiquitination of RIG-I CTD was detected as in (M).

(O) R3T cells were transfected with Riplet, FLAG-tagged RIG-I-CTD, and HA-tagged ubiquitin (HA-Ub) expression vectors. Cells were stimulated with dsRNA. Ubiquitination of RIG-I-CTD was detected as in (M).

See also Figure S3.

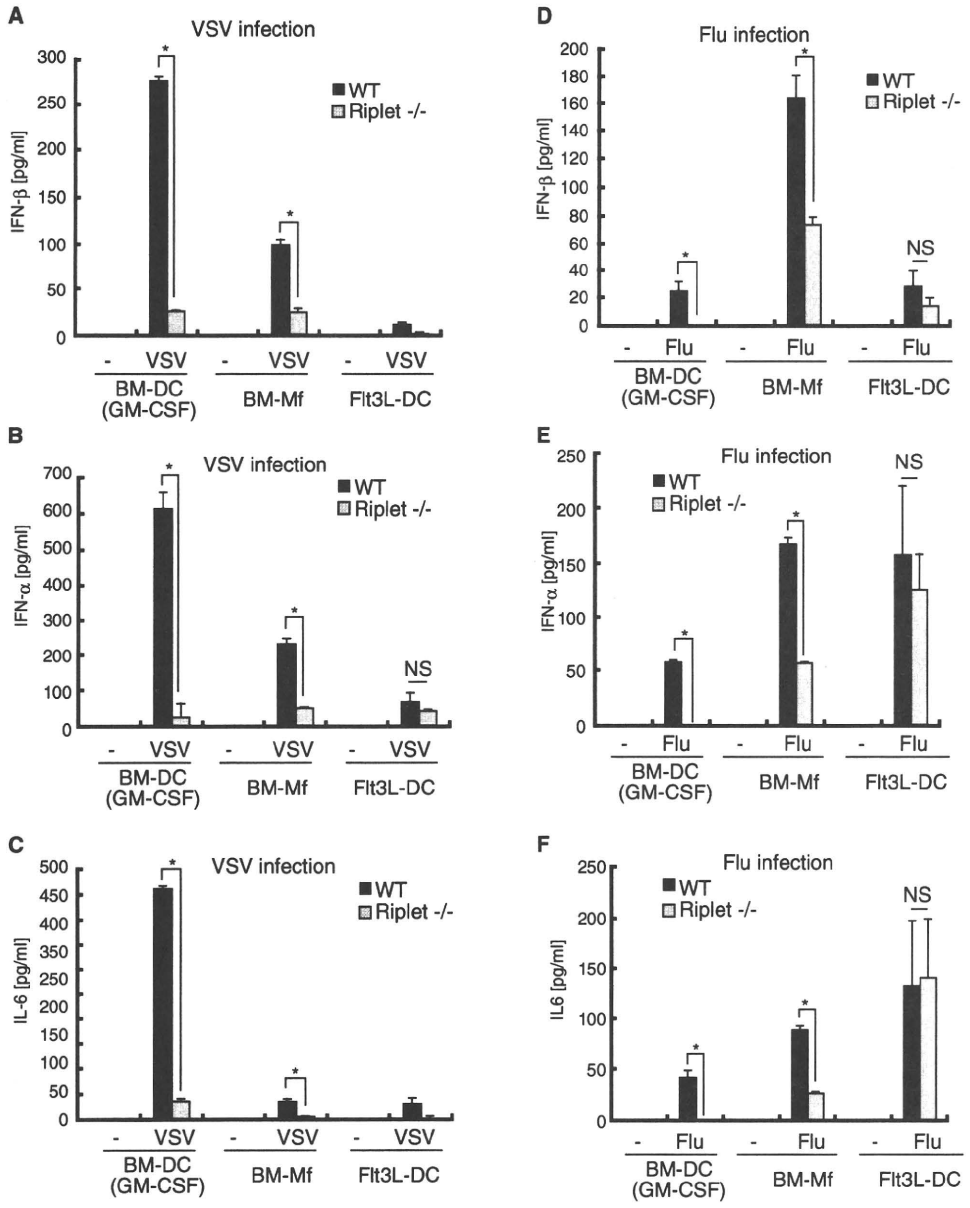

Figure 6. Role of Riplet in Responses to VSV or Flu Infection in Bone Marrow-Derived Cells

GM-DCs, BM-Mf, or Flt3L-DCs were induced from BM-derived cells in the presence of GM-CSF, M-CSF, or Flt3L and infected with VSV or influenza A virus at moi = 1. Twenty-four hours after viral infection, amounts of IFN-β (A and D), -α (B and E), and IL-6 (C and F) in culture supernatants were measured by ELISA. Data are shown as means ±SD and are representative of two independent experiments. *$p < 0.05$ (Student's t test). NS indicates not statistically significant.
See also Figure S4.

by overexpression of Riplet was also abolished by the 5KA mutation. These data support our model. However, we do not exclude the possibility that other Lys residues of RIG-I are ubiquitinated by Riplet, because we have not yet directly detected polyubiquitinated residues of RIG-I CTD by mass spectrometory analysis. Further in vitro studies are required to determine the polyubiquitination sites and to reveal precise RIG-I regulatory mechanisms by Riplet-mediated Lys63-linked polyubiquitation.

In general, E3 ubiquitin ligase targets several types of proteins. Therefore, it is possible that Riplet targets other proteins. Previous work has shown that Riplet binds to the Trk-fused gene (TFG) protein (Suzuki et al., 2001). The TFG protein interacts with TANK and NEMO, which are involved in the NF-κB pathway (Miranda et al., 2006). Although NEMO is involved in IPS-1-mediated signaling, RIG-I CARDs- or MDA5-mediated signaling was normal in *Riplet*$^{-/-}$ MEFs. Therefore, interaction between Riplet

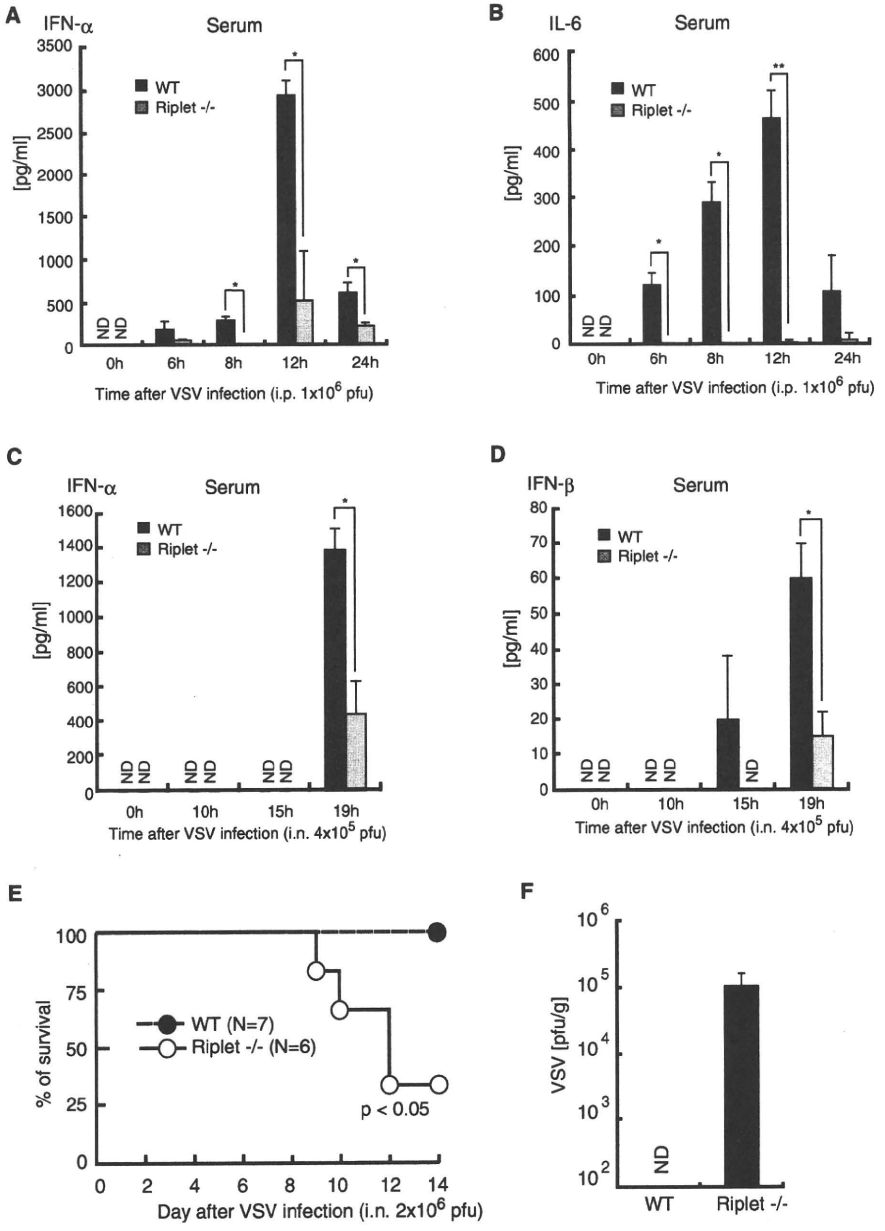

Figure 7. Role of Riplet in Antiviral Responses In Vivo

(A and B) Wild-type or *Riplet*$^{-/-}$ mice were injected intraperitoneally with 1 × 10^6 pfu of VSV. Amounts of IFN-α (A) and IL-6 (B) in mouse serum were measured by ELISA. Data are shown as mean ±SD of samples obtained from three wild-type and three Riplet −/− mice at each time point. *$p < 0.05$ (Student's t test). "ND" indicates not detected.

(C and D) Wild-type and *Riplet*$^{-/-}$ mice were infected intranasally with 4 × 10^5 pfu of VSV. Amounts of IFN-α (C) and IFN-β (D) in mouse serum were measured by ELISA.

(E) Wild-type and *Riplet*$^{-/-}$ mice were infected intranasally with 2 × 10^6 pfu of VSV and mice mortality was observed for 14 days (*$p < 0.05$ between wild-type and *Riplet*$^{-/-}$ mice, log rank test).

(F) Wild-type and *Riplet*$^{-/-}$ mice were infected intranasally with 2 × 10^6 pfu of VSV, and sacrificed for their tissues on day 7 after infection. Titers in brain were determined by the plaque assay. Viral titers in brains of wild-type mice were below 100 pfu/g, and thus not detected (ND). Data are shown as means ±SD (n = 3). See also Figure S5.

and TFG protein is not required for RIG-I-mediated signaling. However, since TFG is involved in tumorigenesis (Miranda et al., 2006), Riplet may be involved in human tumorigenesis.

Several viral proteins inhibit RIG-I-mediated signaling. For example, Flu NS1 inhibits TRIM25 and HCV NS3/4A cleaves IPS-1 (Meylan et al., 2005; Gack et al., 2009). Therefore, Riplet may be inhibited by viral proteins. Indeed, our pilot study indicated that the Riplet protein is disrupted in human hepatocyte cell lines carrying a full-length HCV replicon. RIG-I is involved in innate immune responses against various viruses. In this study, we showed that Riplet is required for innate immune responses against VSV, Flu, and SeV. Therefore, Riplet is also expected to be involved in innate immune responses against other viruses that are recognized by RIG-I.

EXPERIMENTAL PROCEDURES

Generation of Riplet-Deficient Mice

The Riplet gene was amplified by PCR using genomic DNA extracted from ESCs by PCR. The targeting vector was constructed by replacing the second and third exons with a neomycine-resistance gene cassette (Neo), and a herpes simplex virus thymidine kinase (HSV-TK) driven by PGK promoter was inserted into the genomic fragment for negative selection. After the targeting vector was transfected into 129/Sv mice-derived ESCs, G418 and gancyclovir doubly resistant colonies were selected and screened by PCR. The targeted cell line was injected in C57BL/6 blastocysts, resulting in the birth of male chimeric mice. These mice were then crossed with 129/Sv mice to obtain heterozygous mutants. The heterozygous mutants were intercrossed to obtain homozygous *Riplet*$^{-/-}$ mice.

Cells, Viruses, and Reagents

Wild-type and *Riplet*$^{-/-}$ MEFs were prepared from day 12.5–13.5 embryos. *Riplet*$^{-/-}$ MEFs were immortalized with large T antigen and named R3T cell line. BM cells were prepared from 5- to 10-week-old mice. VSV Indiana strain was provided by A. Takada (Hokkaido University). VSV was amplified using Vero cells and the viral titer was determined by the plaque assay. Flu (PR8 strain) and SeV (HVJ strain) was provided by Y. Sakoda (Hokkaido University). HSV-1 strain was provided by K. Kondo (The JIKEI University). Anti-mouse IRF3 antibody was purchased from Zymed. Anti-phospho-STAT1 antibody was purchased from Cell Signaling and anti-STAT1 antibody from Santa Cruz. Salomon sperm dsDNA was purchased from Invitrogen. To determine the viral titer in the brain, the mice were sacrificed, and the brain was aseptically removed and frozen at −80°C. The brain was homogenized in 1 ml of PBS on ice, and the titer was determined by plaque assay.

Preparation of Viral Double-Stranded RNA

cDNA of the HCV 3′UTR region was amplified from total RNA of the HCV genotype 1b full-length replicon using primers HCV-F1 and HCV-R1, and then cloned in the pGEM-T Easy Vector. The primer set sequences were HCV-F1, CTCCAGGTGAGATCAATAGG; and HCV-R1, CGTGACTAGGGCTAAGATGG. RNA was synthesized using T7 and SP6 RNA polymerases. Template DNA was digested by DNase I, and RNA was purified using TRIZOL (Invitrogen) according to manufacturer's instructions.

Quantitative PCR

For qPCR, total RNA was extracted with TRIZOL (Invitrogen) and 0.5 μg of RNA was reverse-transcribed using the High Capacity cDNA Transcription Kit (ABI) with random primers according to the manufacturer's instructions. qPCR was performed using the Step One Real-Time PCR system (ABI). Primer sequences used for qPCR are listed in Table S1.

Measurement of Cytokines

In brief, 5 × 10^5 cells in a 24-well plate were either infected with VSV or Flu, stimulated with LPS, or transfected with HCV 3′UTR dsRNA or poly(I:C). Twenty-four hours after infection, stimulation, or transfection, culture supernatants were collected and analyzed for IFN-α, -β, and IL-6 production by ELISA. Cytokine levels were measured in mouse serum obtained from the mouse tail vein. ELISA kits for mouse IFN-α and -β were purchased from PBL Biomedical Laboratories. ELSA kit for mouse IL-6 was purchased from Invitrogen.

Preparation of Dendritic Cells and Macrophages

BM cells were prepared from the femur and tibia. The cells were cultured in RPMI1640 medium supplemented with 10% FCS, 100 μM 2-Me, and 100 ng/ml human Flt3 ligand (Pepro Tech), and 10 ng/ml murine GM-CSF or culture supernatant NIH 3T3 expressing M-CSF. After 6 days, cells were collected and used as Flt3L-DC, GM-DC, or BM-Mf. In the case of GM-DC or BM-Mf, the medium was changed every 2 days.

Native PAGE Analysis

Approximately 1 × 10^6 MEFs were infected with VSV at moi = 1 for 9 hr and then lysed. Cell lysates in native PAGE sample buffer (62.5 mM Tris-HCl [pH 6.8], 15% glycerol, and BPB) were separated using native PAGE and then immunoblotted with anti-murine IRF3 antibody (Zymed).

Luciferase Assay

Expression plasmids for mouse RIG-I N-terminal CARDs, full-length RIG-I, or full-length MDA5 were constructed in pEF-BOS. The cDNA fragment encoding the ORF of RIG-I or MDA5 was amplified by RT-PCR using total RNA prepared from MEFs. The Riplet dRING mutant protein lacks 1–69 aa region. Wild-type and mutant (Riplet dRING) Riplet-expression vectors were described previously (Oshiumi et al., 2009). Wild-type or *Riplet*$^{-/-}$ MEFs were transiently transfected in 24-well plates with reporter constructs containing the IFN-β promoter and Renilla luciferase (internal control) together with the empty vector (control), RIG-I CARDs, full-length RIG-I, or MDA5 expression vectors. Twenty-four hours after transfection, cells were lysed and subjected to the luciferase assay using the Dual-Luciferase Reporter Assay system (Promega).

Statistical Analyses

Statistical significance of differences between groups was determined by the Student's t test, and survival curves were analyzed by the log rank test using Prism 4 for Macintosh software (GraphPad Sofware, Inc.). Chi-square goodness-of-fit tests and Student's t tests were performed using MS-Excel software and a chi-square distribution table.

SUPPLEMENTAL INFORMATION

Supplemental Information includes five figures, one table, and Supplemental Experimental Procedures and can be found with this article at doi:10.1016/j.chom.2010.11.008.

ACKNOWLEDGMENTS

We thank Dr. John P. Atkinson (Washington University) and Dr. Ralph Steinman (Rockefeller University) for critical discussions, Yoko Esaki and Kiyo Kawata for technical support in generating Riplet KO mice, N. Irie for a pilot study of B-DNA stimulation assay, and Sakoda Y. for technical instructions for the experiments using Flu and SeV. This work was supported in part by the Mitsubishi Foundation; Mochida Foundation; Akiyama Life Science Foundation; and Grants-in-Aid from Ministry of Education, Science, and Culture and Ministry of Health, Labor, and Welfare of Japan.

Received: June 4, 2010
Revised: August 18, 2010
Accepted: November 5, 2010
Published: December 15, 2010

REFERENCES

Akira, S., Uematsu, S., and Takeuchi, O. (2006). Pathogen recognition and innate immunity. Cell *124*, 783–801.

Arimoto, K., Takahashi, H., Hishiki, T., Konishi, H., Fujita, T., and Shimotohno, K. (2007). Negative regulation of the RIG-I signaling by the ubiquitin ligase RNF125. Proc. Natl. Acad. Sci. USA *104*, 7500–7505.

Chiu, Y.H., Macmillan, J.B., and Chen, Z.J. (2009). RNA polymerase III detects cytosolic DNA and induces type I interferons through the RIG-I pathway. Cell *138*, 576–591.

Cui, S., Eisenacher, K., Kirchhofer, A., Brzozka, K., Lammens, A., Lammens, K., Fujita, T., Conzelmann, K.K., Krug, A., and Hopfner, K.P. (2008). The C-terminal regulatory domain is the RNA 5′-triphosphate sensor of RIG-I. Mol. Cell *29*, 169–179.

Diebold, S.S., Kaisho, T., Hemmi, H., Akira, S., and Reis e Sousa, C. (2004). Innate antiviral responses by means of TLR7-mediated recognition of single-stranded RNA. Science *303*, 1529–1531.

Douglas, J., Cilliers, D., Coleman, K., Tatton-Brown, K., Barker, K., Bernhard, B., Burn, J., Huson, S., Josifova, D., Lacombe, D., et al. (2007). Mutations in RNF135, a gene within the NF1 microdeletion region, cause phenotypic abnormalities including overgrowth. Nat. Genet. *39*, 963–965.

Gack, M.U., Shin, Y.C., Joo, C.H., Urano, T., Liang, C., Sun, L., Takeuchi, O., Akira, S., Chen, Z., Inoue, S., and Jung, J.U. (2007). TRIM25 RING-finger E3 ubiquitin ligase is essential for RIG-I-mediated antiviral activity. Nature *446*, 916–920.

Gack, M.U., Kirchhofer, A., Shin, Y.C., Inn, K.S., Liang, C., Cui, S., Myong, S., Ha, T., Hopfner, K.P., and Jung, J.U. (2008). Roles of RIG-I N-terminal tandem CARD and splice variant in TRIM25-mediated antiviral signal transduction. Proc. Natl. Acad. Sci. USA *105*, 16743–16748.

Gack, M.U., Albrecht, R.A., Urano, T., Inn, K.S., Huang, I.C., Carnero, E., Farzan, M., Inoue, S., Jung, J.U., and Garcia-Sastre, A. (2009). Influenza A virus NS1 targets the ubiquitin ligase TRIM25 to evade recognition by the host viral RNA sensor RIG-I. Cell Host Microbe *5*, 439–449.

Gao, D., Yang, Y.K., Wang, R.P., Zhou, X., Diao, F.C., Li, M.D., Zhai, Z.H., Jiang, Z.F., and Chen, D.Y. (2009). REUL is a novel E3 ubiquitin ligase and stimulator of retinoic-acid-inducible gene-I. PLoS ONE *4*, e5760. 10.1371/journal.pone.0005760.

Honda, K., Yanai, H., Takaoka, A., and Taniguchi, T. (2005). Regulation of the type I IFN induction: a current view. Int. Immunol. *17*, 1367–1378.

Honda, K., Takaoka, A., and Taniguchi, T. (2006). Type I interferon [corrected] gene induction by the interferon regulatory factor family of transcription factors. Immunity *25*, 349–360.

Horner, S.M., and Gale, M., Jr. (2009). Intracellular innate immune cascades and interferon defenses that control hepatitis C virus. J. Interferon Cytokine Res. *29*, 489–498.

Hornung, V., Ellegast, J., Kim, S., Brzozka, K., Jung, A., Kato, H., Poeck, H., Akira, S., Conzelmann, K.K., Schlee, M., et al. (2006). 5′-Triphosphate RNA is the ligand for RIG-I. Science *314*, 994–997.

Ishii, K.J., Coban, C., Kato, H., Takahashi, K., Torii, Y., Takeshita, F., Ludwig, H., Sutter, G., Suzuki, K., Hemmi, H., et al. (2006). A Toll-like receptor-independent antiviral response induced by double-stranded B-form DNA. Nat. Immunol. *7*, 40–48.

Ishii, K.J., Kawagoe, T., Koyama, S., Matsui, K., Kumar, H., Kawai, T., Uematsu, S., Takeuchi, O., Takeshita, F., Coban, C., and Akira, S. (2008). TANK-binding kinase-1 delineates innate and adaptive immune responses to DNA vaccines. Nature *451*, 725–729.

Ishikawa, H., and Barber, G.N. (2008). STING is an endoplasmic reticulum adaptor that facilitates innate immune signalling. Nature *455*, 674–678.

Ishikawa, H., Ma, Z., and Barber, G.N. (2009). STING regulates intracellular DNA-mediated, type I interferon-dependent innate immunity. Nature *461*, 788–792.

Kato, H., Sato, S., Yoneyama, M., Yamamoto, M., Uematsu, S., Matsui, K., Tsujimura, T., Takeda, K., Fujita, T., Takeuchi, O., and Akira, S. (2005). Cell type-specific involvement of RIG-I in antiviral response. Immunity *23*, 19–28.

Kato, H., Takeuchi, O., Sato, S., Yoneyama, M., Yamamoto, M., Matsui, K., Uematsu, S., Jung, A., Kawai, T., Ishii, K.J., et al. (2006). Differential roles of MDA5 and RIG-I helicases in the recognition of RNA viruses. Nature *441*, 101–105.

Kawai, T., Takahashi, K., Sato, S., Coban, C., Kumar, H., Kato, H., Ishii, K.J., Takeuchi, O., and Akira, S. (2005). IPS-1, an adaptor triggering RIG-I- and Mda5-mediated type I interferon induction. Nat. Immunol. *6*, 981–988.

Kumagai, Y., Takeuchi, O., Kato, H., Kumar, H., Matsui, K., Morii, E., Aozasa, K., Kawai, T., and Akira, S. (2007). Alveolar macrophages are the primary interferon-alpha producer in pulmonary infection with RNA viruses. Immunity *27*, 240–252.

Kumar, H., Kawai, T., Kato, H., Sato, S., Takahashi, K., Coban, C., Yamamoto, M., Uematsu, S., Ishii, K.J., Takeuchi, O., and Akira, S. (2006). Essential role of IPS-1 in innate immune responses against RNA viruses. J. Exp. Med. *203*, 1795–1803.

Meylan, E., Curran, J., Hofmann, K., Moradpour, D., Binder, M., Bartenschlager, R., and Tschopp, J. (2005). Cardif is an adaptor protein in the RIG-I antiviral pathway and is targeted by hepatitis C virus. Nature *437*, 1167–1172.

Miranda, C., Roccato, E., Raho, G., Pagliardini, S., Pierotti, M.A., and Greco, A. (2006). The TFG protein, involved in oncogenic rearrangements, interacts with TANK and NEMO, two proteins involved in the NF-kappaB pathway. J. Cell. Physiol. *208*, 154–160.

Nakhaei, P., Genin, P., Civas, A., and Hiscott, J. (2009). RIG-I-like receptors: sensing and responding to RNA virus infection. Semin. Immunol. *21*, 215–222.

Onoguchi, K., Yoneyama, M., Takemura, A., Akira, S., Taniguchi, T., Namiki, H., and Fujita, T. (2007). Viral infections activate types I and III interferon genes through a common mechanism. J. Biol. Chem. *282*, 7576–7581.

Oshiumi, H., Matsumoto, M., Hatakeyama, S., and Seya, T. (2009). Riplet/RNF135, a RING finger protein, ubiquitinates RIG-I to promote interferon-beta induction during the early phase of viral infection. J. Biol. Chem. *284*, 807–817.

Pichlmair, A., Schulz, O., Tan, C.P., Naslund, T.I., Liljestrom, P., Weber, F., and Reis e Sousa, C. (2006). RIG-I-mediated antiviral responses to single-stranded RNA bearing 5′-phosphates. Science *314*, 997–1001.

Rehwinkel, J., Tan, C.P., Goubau, D., Schulz, O., Pichlmair, A., Bier, K., Robb, N., Vreede, F., Barclay, W., Fodor, E., and Reis e Sousa, C. (2010). RIG-I detects viral genomic RNA during negative-strand RNA virus infection. Cell *140*, 397–408.

Saito, T., Hirai, R., Loo, Y.M., Owen, D., Johnson, C.L., Sinha, S.C., Akira, S., Fujita, T., and Gale, M., Jr. (2007). Regulation of innate antiviral defenses through a shared repressor domain in RIG-I and LGP2. Proc. Natl. Acad. Sci. USA *104*, 582–587.

Saito, T., Owen, D.M., Jiang, F., Marcotrigiano, J., and Gale, M., Jr. (2008). Innate immunity induced by composition-dependent RIG-I recognition of hepatitis C virus RNA. Nature *454*, 523–527.

Seth, R.B., Sun, L., Ea, C.K., and Chen, Z.J. (2005). Identification and characterization of MAVS, a mitochondrial antiviral signaling protein that activates NF-kappaB and IRF 3. Cell *122*, 669–682.

Shigemoto, T., Kageyama, M., Hirai, R., Zheng, J., Yoneyama, M., and Fujita, T. (2009). Identification of loss of function mutations in human genes encoding RIG-I and MDA5: implications for resistance to type I diabetes. J. Biol. Chem. *284*, 13348–13354.

Sun, Q., Sun, L., Liu, H.H., Chen, X., Seth, R.B., Forman, J., and Chen, Z.J. (2006). The specific and essential role of MAVS in antiviral innate immune responses. Immunity *24*, 633–642.

Suzuki, H., Fukunishi, Y., Kagawa, I., Saito, R., Oda, H., Endo, T., Kondo, S., Bono, H., Okazaki, Y., and Hayashizaki, Y. (2001). Protein-protein interaction panel using mouse full-length cDNAs. Genome Res. *11*, 1758–1765.

Takahasi, K., Yoneyama, M., Nishihori, T., Hirai, R., Kumeta, H., Narita, R., Gale, M., Jr., Inagaki, F., and Fujita, T. (2008). Nonself RNA-sensing mechanism of RIG-I helicase and activation of antiviral immune responses. Mol. Cell *29*, 428–440.

Takeuchi, O., and Akira, S. (2010). Pattern recognition receptors and inflammation. Cell *140*, 805–820.

Xu, L.G., Wang, Y.Y., Han, K.J., Li, L.Y., Zhai, Z., and Shu, H.B. (2005). VISA is an adapter protein required for virus-triggered IFN-beta signaling. Mol. Cell *19*, 727–740.

Yoneyama, M., and Fujita, T. (2009). RNA recognition and signal transduction by RIG-I-like receptors. Immunol. Rev. *227*, 54–65.

Yoneyama, M., and Fujita, T. (2010). Recognition of viral nucleic acids in innate immunity. Rev. Med. Virol. *20*, 4–22.

Yoneyama, M., Kikuchi, M., Natsukawa, T., Shinobu, N., Imaizumi, T., Miyagishi, M., Taira, K., Akira, S., and Fujita, T. (2004). The RNA helicase RIG-I has an essential function in double-stranded RNA-induced innate antiviral responses. Nat. Immunol. *5*, 730–737.

Zeng, W., Sun, L., Jiang, X., Chen, X., Hou, F., Adhikari, A., Xu, M., and Chen, Z.J. (2010). Reconstitution of the RIG-I pathway reveals a signaling role of unanchored polyubiquitin chains in innate immunity. Cell *141*, 315–330.

THE JOURNAL OF BIOLOGICAL CHEMISTRY VOL. 285, NO. 26, pp. 20128–20136, June 25, 2010

A Molecular Mechanism for Toll-IL-1 Receptor Domain-containing Adaptor Molecule-1-mediated IRF-3 Activation*[S]

Received for publication, December 24, 2009, and in revised form, March 25, 2010 Published, JBC Papers in Press, April 23, 2010, DOI 10.1074/jbc.M109.099101

Megumi Tatematsu[‡], Akihiro Ishii[‡1], Hiroyuki Oshiumi[‡], Masataka Horiuchi[§], Fuyuhiko Inagaki[§], Tsukasa Seya[‡], and Misako Matsumoto[‡2]

From the [‡]Department of Microbiology and Immunology, Hokkaido University Graduate School of Medicine, Kita 15, Nishi 7, Kita-ku, Sapporo 060-8638 and the [§]Department of Structural Biology, Graduate School of Pharmaceutical Science, Hokkaido University, N-21, W-11, Kita-ku, Sapporo 001-0021, Japan

The Toll-IL-1 receptor (TIR) domain-containing adaptor molecule-1 (TICAM-1, also called TRIF) is a signaling adaptor for TLR3 and TLR4 that activates the transcription factors IRF-3, NF-κB, and AP-1, leading to induction of type I interferon and cytokines. The N-terminal region of TICAM-1 participates in IRF-3 activation, although the C-terminal region is involved in NF-κB activation. However, the mechanism by which TICAM-1 is activated and transmits signals is largely unknown. In this study, we identified Leu^{194} as a critical amino acid for TICAM-1-mediated IRF-3 activation. When Leu^{194} was substituted with Ala, the mutant TICAM-1 failed to recruit the IRF-3 kinase TBK1, resulting in lack of IRF-3 phosphorylation, although TRAF3 and NAP1 appeared to be recruited. The N-terminal 176 amino acids of TICAM-1 (N-terminal domain (NTD)) form a protease-resistant structural domain. A TICAM-1 mutant lacking the N-terminal 180 amino acids showed greater interferon-β promoter activation than wild-type TICAM-1. Furthermore, immunoprecipitation and protein-protein interaction analysis revealed that the NTD interacted with the N terminus of TICAM-1-TIR. These results suggest that the NTD folds into the TIR domain structure to maintain the naive conformation of TICAM-1. Upon stimulation of TLR3/4, TICAM-1 oligomerizes through the TIR domain and the C-terminal region, which may break the intramolecular association and induce a conformational change that allows TBK1 access to TICAM-1.

The innate immune system senses microbial infection using Toll-like receptors and cytoplasmic pattern-recognition receptors, which rapidly induce an antimicrobial response (1). Recent studies have demonstrated that these receptors also recognize molecular patterns associated with tissue damage and induce cytokine and chemokine production, which may lead to a sterile inflammation and progression of autoimmune diseases (2). Downstream of each pattern-recognition receptor is a signaling adaptor protein that determines the nature of response by activating distinct transcription factors (3). The Toll-IL-1 receptor (TIR)[3] domain-containing adaptor molecule-1 (TICAM-1), which is also known as TIR domain-containing adaptor inducing IFN-β (TRIF), is a signaling adaptor for TLR3 and TLR4 that activates the transcription factors IRF-3, NF-κB, and AP-1, leading to induction of type I IFN and cytokines, as well as myeloid dendritic cell (mDC) maturation (4–7). The final response mediated by TICAM-1 depends on the cell type and the activating TLR3/4 ligand.

Poly(I-C) is a synthetic analog of viral double strand RNA that generates a unique maturation stage in mDCs via TLR3-TICAM-1-dependent gene expression, leading to activation of natural killer cells and cytotoxic T lymphocytes (8, 9). Monophosphoryl lipid A is a TLR4 ligand that activates mDCs to induce T cell immunity via TICAM-1 but not MyD88 (10), implying that TICAM-1 signaling is crucial for inducing effective cellular responses. In contrast, oxidized phospholipids generated by oxidative stress or virus infection activate cytokine production in lung macrophages through the TLR4-TICAM-1 pathway, and this is the key disease pathway in acute lung injury (11). Thus, specific stimuli have been discovered, but the mechanism by which TICAM-1 is activated by upstream pattern-recognition receptors and transmits downstream signals is largely unknown.

TICAM-1 is expressed at a low level in most tissues and cells and is diffusely localized in the cytoplasm of resting cells (4, 12). When endosomal TLR3 is activated by double strand RNA, TICAM-1 transiently colocalizes with TLR3 and then dissociates from the receptor and forms speckled structures that colocalize with downstream signaling molecules (12, 13). Upon

* This work was supported in part by grants-in-aid from the Ministry of Education, Science, and Culture, the Ministry of Health, Labor, and Welfare of Japan, The NorthTec Foundation, The Akiyama Life Science Foundation, Sapporo Biocluster "Bio-S" (Knowledge Cluster Initiative of Ministry of Education, Culture, Sports, Science and Technology), and the Program of Founding Research Centers for Emerging and Reemerging Infectious Diseases, Ministry of Education, Culture, Sports, Science and Technology.

[S] The on-line version of this article (available at http://www.jbc.org) contains supplemental Figs. 1 and 2.

[1] Present address: Dept. of Global Epidemiology, Hokkaido University Research Center for Zoonosis Control, Kita-20, Nishi-10, Kita-ku, Sapporo, 001-0020, Japan.

[2] To whom correspondence should be addressed. Tel.: 81-11-706-6056; Fax: 81-11-706-7866; E-mail: matumoto@pop.med.hokudai.ac.jp.

[3] The abbreviations used are: TIR, Toll-IL-1 receptor; DAPI, 4′,6-diamidine-2′-phenylindole dihydrochloride; mDC, myeloid dendritic cell; NTD, N-terminal domain (1–176 aa); RHIM, RIP homotypic interacting motif; TRAF, tumor necrosis factor receptor-associated factor; TRIF, TIR domain-containing adaptor-inducing IFN-β; aa, amino acid; PBS, phosphate-buffered saline; HA, hemagglutinin; IFN, interferon; Ab, antibody; mAb, monoclonal antibody; pAb, polyclonal antibody.

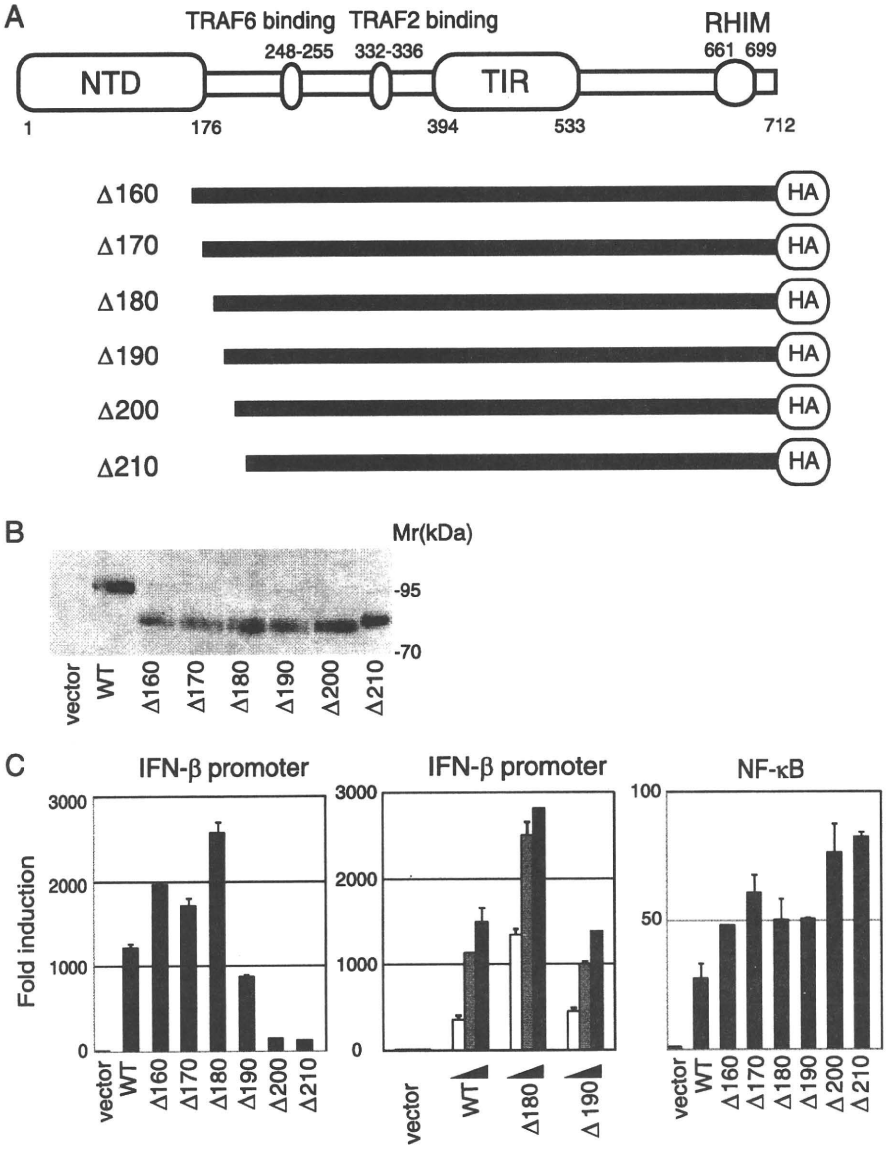

FIGURE 1. **TICAM-1 N-terminal region (191–200 aa) is essential for activation of the IFN-β promoter but not NF-κB.** *A*, schematic structure of human TICAM-1/TRIF and TICAM-1 mutants. *B*, protein expression of truncated TICAM-1 mutants in HEK293 cells. HEK293 cells in 24-well plates were transfected with the expression plasmids for HA-tagged wild-type TICAM-1 or TICAM-1 mutants (100 ng). Protein expression levels were determined by immunoblotting using anti-HA pAb. *C*, functional analysis of TICAM-1 mutants. HEK293 cells were transfected with empty vector or expression plasmid for wild-type (*WT*) TICAM-1 or each TICAM-1 mutant (Δ160–Δ210) (100 ng) together with the IFN-β promoter reporter (*left panel*) or NF-κB reporter plasmid (*right panel*), and phRL-TK. In some experiments, HEK293 cells were transfected with increasing amounts of expression vectors (10, 50, and 100 ng) (*center panel*). Luciferase activity was measured 24 h after transfection. Representative data from a minimum of four separate experiments, each performed in triplicate, are shown.

lipopolysaccharide stimulation, TICAM-1 is activated by endosomal TICAM-2 (also called TRIF-related adaptor molecule), which associates with the internalized TLR4 (14). Forced expression of TICAM-1 leads to homo-oligomerization through the TIR domain and the C terminus, forming a complex called the TICAM-1 signalosome (15). The TIR domain of TICAM-1 is essential for binding to the TIR domain of TLR3 and to TICAM-2. The N-terminal region of TICAM-1 participates in IRF-3 activation by recruiting the IRF-3-activating kinases, TANK-binding kinase 1 (TBK1) and inhibitor of nuclear factor κB kinase ϵ (also called IKKι) (16–18). The C-terminal region of TICAM-1 is involved in NF-κB activation and inducing apoptosis by binding the RIP1 at the receptor-interacting protein homotypic interacting motif (RHIM) domain (19, 20). The tumor necrosis factor receptor-associated factor (TRAF) 3 and NF-κB-activating kinase-associated protein 1 (NAP1) engage in TICAM-1-mediated activation of IRF-3 (21–23). Thus, although molecules involved in the TICAM-1-mediated signaling have been identified, the molecular mechanism for TICAM-1 activation remains unknown.

Recently, the N-terminal 176 amino acids (aa) of TICAM-1 (NTD) were found to form a protease-resistant structure of eight α-helices (24). In this study, we analyzed the structure-function relationship of TICAM-1 with a series of TICAM-1 mutants and identified the critical amino acid for TICAM-1-mediated IRF-3 activation. Moreover, we offer a structural model of the resting form of TICAM-1, in which NTD folds into the TIR domain structure, preventing homodimerization and access of downstream signaling molecules to TICAM-1.

EXPERIMENTAL PROCEDURES

Cell Culture and Reagents—HEK293 cells were maintained in Dulbecco's modified Eagle's medium low glucose (Invitrogen) supplemented with 10% heat-inactivated fetal calf serum (BIOSOURCE) and antibiotics. HEK293FT cells were maintained in Dulbecco's modified Eagle's medium high glucose supplemented with 0.1 mM nonessential amino acids, 10% heat-inactivated fetal calf serum, and antibiotics. HeLa cells were maintained in minimum essential media (Nissui, Tokyo, Japan) supplemented with 1% L-glutamine and 5% heat-inactivated fetal calf serum. Anti-FLAG M2 mAb, anti-HA pAb, 4′,6-diamidine-2′-phenylindole dihydrochloride (DAPI), and benzyloxycarbonyl-VAD-fluoromethyl ketone were from Sigma. Alexa Fluor®-conjugated secondary antibodies were from Invitrogen; anti-Myc mAb was from Neomarkers (Lab Vision

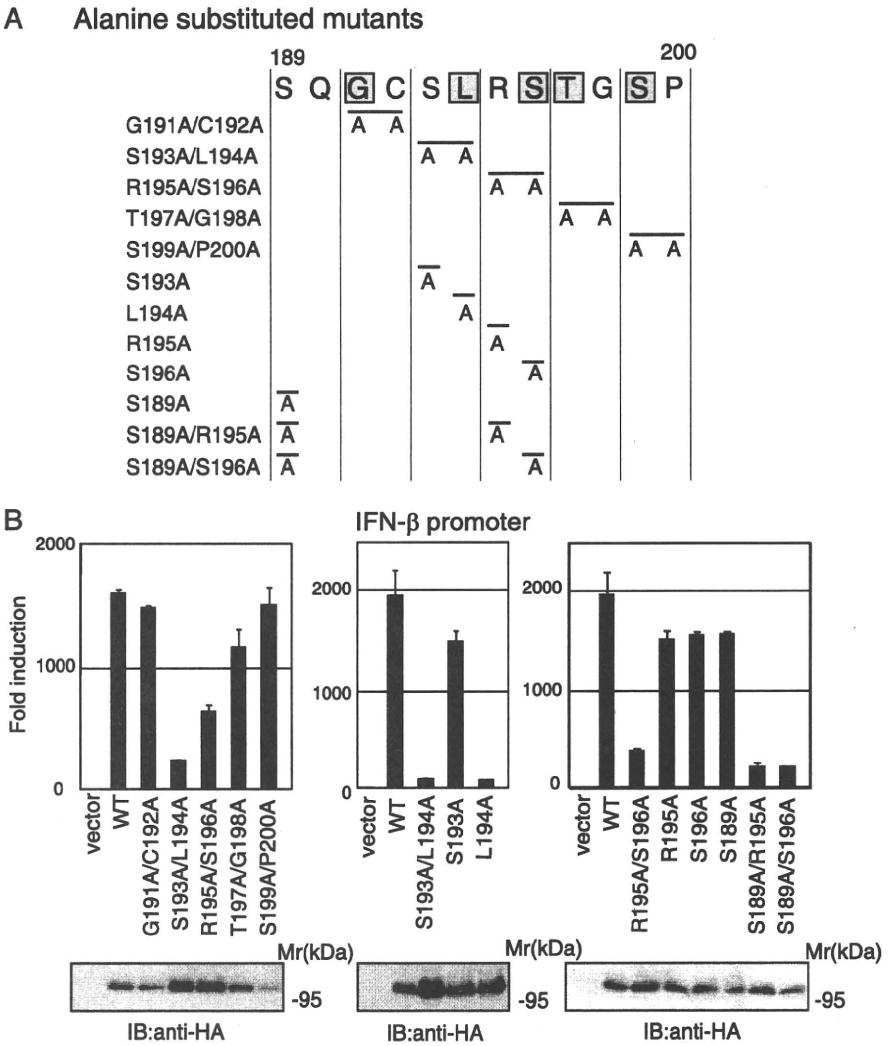

FIGURE 2. **Leu[194] is critical for TICAM-1-mediated IFN-β promoter activation.** *A*, amino acid sequence between Ser[189] and Pro[200] in TICAM-1. *Gray* indicates conserved residues between human and mouse. *B*, IFN-β promoter activation by alanine-substituted TICAM-1 mutants. HEK293 cells were transfected with empty vector or expression vectors for wild-type (*WT*) TICAM-1 or indicated alanine-substituted mutants, with the IFN-β promoter reporter and phRL-TK. Luciferase activity was measured 24 h after transfection. Representative data from a minimum of three separate experiments, each performed in triplicate, are shown. *Lower panels*, protein expression of alanine-substituted mutants in HEK293 cells. Cell lysates prepared in *A* were subjected to SDS-PAGE (7.5% gel) followed by immunoblotting (*IB*) with anti-HA pAb.

Corp., Fremont, CA); anti-HA mAb was from Covance (Emeryville, CA); anti-TBK1 pAb was from Abcam (Cambridge, MA); anti-human IRF3 rabbit IgG was from IBL (Gunma, Japan); horseradish peroxidase-conjugated secondary Abs were from BIOSOURCE; and poly(I-C) was from GE Healthcare.

Plasmids—Complementary DNAs for human TICAM-1, RIP1, TRAF2, TRAF3, and TRAF6 were cloned in our laboratory by reverse transcription-PCR and ligated into the cloning site of the expression vectors, pEF-BOS and p3×FLAG-CMV-14 (C-terminal 3×FLAG tag) (15). The pCDNA3.1/NAP1-Myc and pCDNA3.1/TBK1-FLAG expression vectors were kindly provided by Dr. M. Nakanishi (Nagoya City University, Nagoya, Japan). N-terminal deletion mutants of TICAM-1 (Δ160, Δ170, Δ180, Δ190, Δ200, and Δ210) were made by PCR with *Pfu* Turbo DNA polymerase (Stratagene, La Jolla, CA) using appropriate primers. pEF-BOS/TICAM-1-HA was used as a PCR template (33). Point mutations in TICAM-1 were generated by site-directed mutagenesis. Truncated TICAM-1 mutants TICAM-1-NTD (1–176 aa), TICAM-1-N (1–359 aa), TICAM-1-TIR (387–556 aa), and TICAM-1-C (534–712 aa) were generated by PCR using specific primers. An HA tag was inserted at the C terminus of each mutant.

Reporter Gene Assays—HEK293 cells (2×10^5 cells/well) cultured in 24-well plates were transfected with expression vectors for wild-type TICAM-1, TICAM-1 mutants, or empty vector, together with the reporter plasmid (100 ng/well) and an internal control vector, phRL-TK (Promega, Madison, WI) (5 ng/well) using FuGENE HD (Roche Diagnostics). The p-125 luciferase reporter contained the human IFN-β promoter (−125 to +19) and was provided by Dr. T. Taniguchi (University of Tokyo, Tokyo, Japan). A luciferase-linked NF-κB reporter gene and pAP-1-Luc reporter plasmid were from Stratagene. The total amount of DNA (500 ng/well) was kept constant by adding empty vector. After 24 h, cells were lysed in lysis buffer (Promega), and firefly and *Renilla* luciferase activities were determined using a Dual-Luciferase reporter assay kit (Promega). The firefly luciferase activity was normalized to the *Renilla* activity and expressed as the fold-stimulation relative to the activity of vector-transfected cells. All assays were performed in triplicate.

Confocal Microscopy—HeLa cells (1.0×10^5 cells/well) were plated onto micro cover glasses (Matsunami, Tokyo, Japan) in 12-well plates. The next day, cells were transfected with the indicated plasmids as above. For cells transfected with wild-type TICAM-1 or the L194A mutant, benzyloxycarbonyl-VAD-fluoromethyl ketone (20 μM) was added to the cells before transfection to inhibit apoptosis. 24 h after transfection, cells were fixed in acetone for 3 min and permeabilized with PBS containing 0.2% Triton X-100 for 10 min. Fixed cells were blocked in phosphate-buffered saline (PBS) containing 1% bovine serum albumin and labeled with the indicated primary Abs (3.0 μg/ml) for 60 min at room temperature. For staining endogenous TBK1, cells were fixed with 4% paraformaldehyde

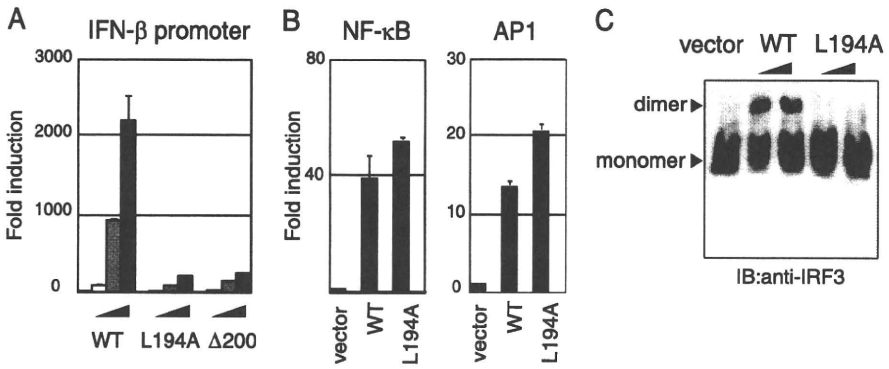

FIGURE 3. **Leu[194] is critical for TICAM-1-mediated IRF-3 activation.** *A*, L194A mutant lost IFN-β promoter-activating ability. HEK293 cells were transfected with increasing amounts of wild-type (*WT*) TICAM-1 or L194A mutant expression vector (1, 10, and 100 ng) with an IFN-β reporter and phRL-TK. Luciferase activity was measured 24 h after transfection. Representative data from a minimum of three separate experiments are shown. *B*, L194A mutant activates NF-κB and AP-1. HEK293 cells were transfected with wild-type TICAM-1 or L194A mutant expression vector (100 ng) together with NF-κB (*left panel*) or AP-1 (*right panel*) reporters. *C*, L194A lost IRF-3 activating ability. HEK293 cells were transfected with empty vector, wild-type TICAM-1 vector, or L194A vector (100 and 400 ng). After 24 h, lysates were prepared and subjected to native PAGE. Monomeric and dimeric forms of IRF-3 (*arrowheads*) were detected by Western blot. *IB*, immunoblot.

for 10 min. Endogenous TBK1 was labeled with anti-TBK1 pAb (1:500). Alexa Fluor 488- or 594-conjugated secondary Abs (1:400) were used to visualize the primary Abs. Nuclei were stained with DAPI (2 μg/ml) in PBS for 10 min before mounting onto glass slides using PBS with 2.3% 1,4-diazabicyclo[2.2.2]octane and 50% glycerol. Cells were visualized at a 63× magnification with an LSM510 META microscope (Zeiss, Jena, Germany).

Immunoprecipitation and Immunoblotting—HEK293FT cells (5×10^5 cells/well) cultured in 6-well plates were transfected as above with the indicated plasmids. For wild-type TICAM-1 and the TICAM-1 mutants containing the RHIM domain, benzyloxycarbonyl-VAD-fluoromethyl ketone (20 μM) was added as described above. The total amount of DNA (2.0 μg/well) was kept constant with an empty vector. After 24 h, cells were lysed in lysis buffer (20 mM Tris-HCl, pH 7.5, containing 150 mM NaCl, 1% Nonidet P-40, 10 mM EDTA, 25 mM iodoacetamide, 2 mM phenylmethylsulfonyl fluoride, 5 mM Na_3VO_4 and a protease inhibitor mixture (Roche Diagnostics)). Lysates were pre-cleared with protein G-Sepharose (GE Healthcare) and incubated with 0.5 μg of anti-tag Abs or anti-TBK1 pAb (1:50). Immunocomplexes were recovered by incubation with protein G-Sepharose, washed five times with lysis buffer, and resuspended in denaturing buffer. Samples were analyzed by SDS-PAGE (7.5–12.5% gel) under reducing conditions followed by immunoblotting with anti-tag Abs. For immunoblotting, HEK293 cells cultured in 24-well plates were transfected with the indicated plasmids (100 ng). After 24 h, cells were lysed in lysis buffer. Lysates were clarified by centrifugation and subjected to SDS-PAGE (7.5% gel) followed by immunoblotting with anti-HA pAb.

Assay for IRF-3 Activation—HEK293 cells (2×10^5 cells/well) cultured in 24-well plates were transfected with wild-type TICAM-1 or TICAM-1 L194A mutant (0.1 and 0.4 μg) using Lipofectamine 2000 reagent (Invitrogen). The total amount of DNA (0.8 μg/well) was kept constant with an empty vector. After 24 h, cells were lysed in lysis buffer (50 mM Tris-HCl, pH 8.0, containing 150 mM NaCl, 1% Nonidet P-40, 100 ng/ml leupeptin, 1 mM phenylmethylsulfonyl fluoride, and 5 mM Na_3VO_4). Lysates were clarified by centrifugation (15,000 rpm, 10 min) and subjected to native-PAGE (7.5% gel) as described previously (34). Immunoblotting was performed using rabbit anti-human IRF-3 antibody and horseradish peroxidase-conjugated goat anti-rabbit IgG.

Protein-Protein Interaction Analysis—Protein-protein association in living cells was analyzed using the *CoralHue* Fluo-chase kit (MBL, Nagoya, Japan), which detects protein-protein interactions as fluorescent signals using the protein fragment complementation method. TICAM-1 NTD and TICAM-1-TIR cDNAs were subcloned into fusion protein expression plasmids according to the manufacturer's instructions. The *TICAM-1* NTD gene was fused to the 3′-end of the divided monomeric Kusabira-Green (*mKG*) gene N- or C-terminal fragment (mKGN-NTD and mKGC-NTD), and the *TICAM-1*-TIR gene was fused to the 5′- or 3′-end of the *mKG* gene N- or C-terminal fragment (TIR-mKGN, TIR-mKGC, mKGN-TIR, and mKGC-TIR). HEK293FT cells (5×10^5 cells/well) cultured in 6-well plates were transfected with the indicated combinations of plasmids as above. After 24 h, the conditioned media were replaced with Dulbecco's PBS, and fluorescent living cells were visualized with fluorescent microscopy (Olympus).

RESULTS

TICAM-1 N Terminus from Gly[191] to Pro[200] Is Essential for IFN-β Promoter Activation—The N terminus of TICAM-1 contains TRAF6- and TRAF2-binding sites (Fig. 1*A*). Limited trypsin digestion of TICAM-1 (1–556 aa) for 4 h generates the N-terminal fragment TICAM-1(1–176), and 20 h of digestion yields the fragment TICAM-1(1–156) (24). To examine the role of the TICAM-1 N-terminal domain, we made a series of truncated constructs (Δ160–Δ210) and assayed NF-κB and IRF-3 activation by reporter assay. The protein expression levels of these mutants were approximately equivalent to wild type (Fig. 1*B*). TICAM-1-mediated IFN-β promoter activation was enhanced by deletion of the N-terminal 160, 170, or 180 aa, whereas the TICAM-1-mutant lacking the N-terminal 190 aa (Δ190) showed less activity than wild-type TICAM-1 (Fig. 1*C*, *left* and *center panels*). Interestingly, a TICAM-1 mutant lacking the N-terminal 200 or 210 aa (Δ200, Δ210) showed dramatic loss of activity. NF-κB activation ability, however, was enhanced in all the mutants (Fig. 1*C*, *right panel*). These results indicated that the N-terminal amino acids between Gly^{191} and Pro^{200} are essential for TICAM-1-mediated IFN-β promoter activation but not for NF-κB activation.

Leu^{194} *Is Critical for TICAM-1-mediated IFN-β Promoter Activation*—To identify residues crucial for TICAM-1-mediated IFN-β promoter activation, we performed alanine scanning of the region between Gly^{191} and Pro^{200} (Fig. 2*A*). Alanine-substituted mutants were expressed in HEK293 cells with an IFN-β reporter gene, and IFN-β promoter activation was assessed after 24 h. Western blot showed that the mutated proteins were expressed at levels similar to wild-type TICAM-1 in HEK293 cells (Fig. 2*B*, *lower panels*). Similar to the Δ200 mutant, the S193A/L194A mutant showed no activity, and the R195A/S196A mutant had partially diminished activity (Fig. 2*B*, *left panel*). Other mutations had no effect on the ability to activate the IFN-β promoter. Because substitution of Ser^{193} and Ser^{196} caused dysfunctional mutants, we made the additional single aa-substituted mutants S193A, L194A, R195A, S196A, and S189A and the combinations S189A/R195A and S189A/S196A, and we examined the role of these residues in TICAM-1 signaling (Fig. 2*A*). Remarkably, the substitution of Leu^{194} with Ala completely abolished IFN-β promoter-activation ability, whereas other single aa substitutions only slightly decreased activity. Both S189A/R195A and S189A/S196A mutants showed severely reduced activity (Fig. 2*B*, *center* and *right panels*). These results suggested that Leu^{194} is a critical amino acid for TICAM-1-mediated IFN-β promoter activation and that Ser^{189}, Arg^{195}, and Ser^{196} near Leu^{194} are associated with this promoter activation.

Leu^{194} *Is Indispensable for TICAM-1-mediated IRF-3 Activation*—The L194A mutant did not activate the IFN-β promoter, even though its expression was comparable with wild-type TICAM-1 (Fig. 3*A*). The promoter of the human IFN-β gene possesses binding sites for IRF-3, NF-κB, and AP-1 (25), so we examined which activation pathways were affected by mutation of Leu^{194}. As shown in Fig. 3*B*, substitution of Leu^{194} with Ala did not affect NF-κB- and AP-1-activation. In contrast, the ability to activate IRF-3 was abolished in the L194A mutant. Phosphorylation and dimer formation of IRF-3 were induced by the forced expression of wild-type TICAM-1 but not the L194A mutant in HEK293 cells (Fig. 3*C*), which suggested that

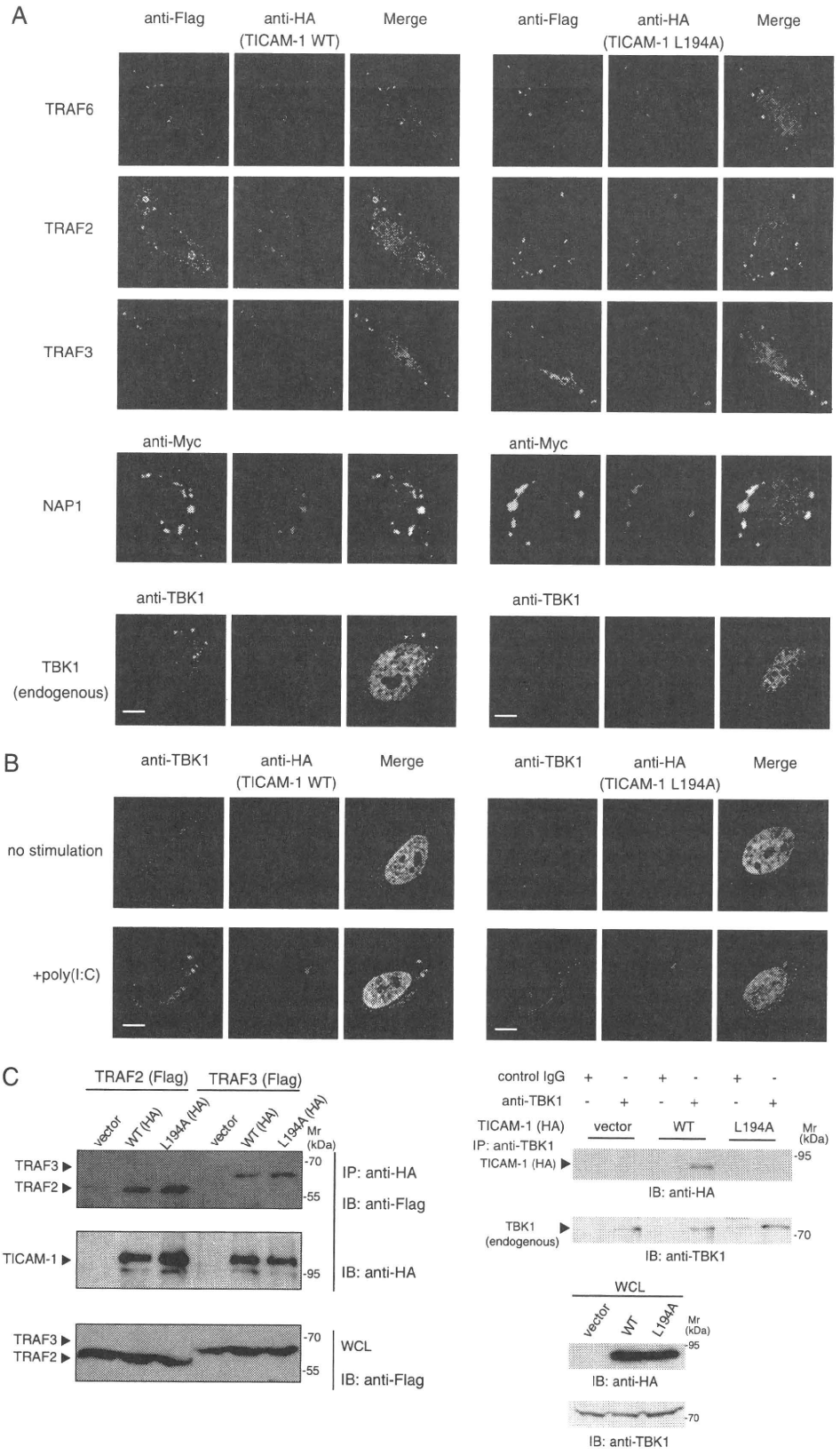

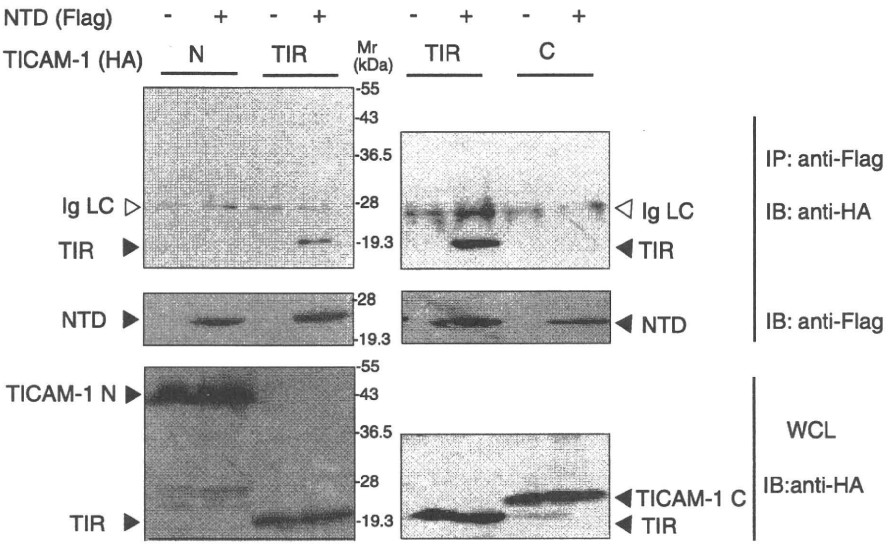

FIGURE 5. **NTD physically associates with TICAM-1-TIR.** HEK293FT cells were transfected with FLAG-tagged NTD and HA-tagged TICAM-1-N (1–359 aa), TIR domain (387–566 aa), or TICAM-1-C (567–712 aa). After 24 h, cells were lysed, and NTD was immunoprecipitated (*IP*) using an anti-FLAG mAb. The immunoprecipitants were resolved on SDS-PAGE (12.5% gel) under reducing conditions followed by immunoblotting (*IB*) with anti-HA pAb or anti-FLAG mAb. Whole cell lysates (*WCL*) were subjected to immunoblotting with anti-HA pAb to detect protein expression. *Open arrowheads* indicate immunoglobulin light chain (*Ig LC*). Molecular weight markers are on the *right*.

Leu^{194} is indispensable for TICAM-1-mediated IRF-3 activation.

Leu^{194} Is a Critical Amino Acid for Recruitment of TBK1 to TICAM-1—TRAF3 is an essential signaling molecule for TICAM-1-mediated IRF-3 activation (22, 23), and TRAF6 and TRAF2 directly bind to the N terminus of TICAM-1 through distinct binding sites (26). We analyzed the recruitment of TRAF family members to wild-type TICAM-1 or the L194A mutant by immunofluorescence staining and confocal microscopy. When HeLa cells were cotransfected with expression plasmids for HA-tagged wild-type or mutated TICAM-1, and FLAG-tagged TRAF6, TRAF2, or TRAF3, TRAF proteins colocalized with the L194A mutant as with the wild type (Fig. 4*A*). These results were confirmed by immunoprecipitation (Fig. 4*C*, *left panel*). We next examined whether Leu^{194} is required for recruitment of NAP1 and TBK1. NAP1, which is essential for TICAM-1-mediated IRF-3 activation and functions downstream of TRAF3, colocalized with both wild-type and the L194A mutant (Fig. 4*A*). However, the IRF-3 kinase TBK1 did not colocalize with the L194A mutant.

The lack of association between the L194A mutant and endogenous TBK1 was also observed in TLR3-mediated activation. Wild-type and the L194A mutant diffusely localized in cytoplasm when expressed at a low level (Fig. 4*B*). After poly(I-C) stimulation, wild-type TICAM-1 formed a speckle-like signalosome where endogenous TBK1 colocalized (Fig. 4*B*, *left panels*). In contrast, the L194A mutant did not recruit TBK1 to its signalosome (Fig. 4*B*, *right panels*). We analyzed physical association of TBK1 with wild-type or the L194A mutant by immunoprecipitation. Overexpressed HA-tagged wild-type TICAM-1 was coimmunoprecipitated with endogenous TBK1, although the L194A mutant was not (Fig. 4*C*, *right panels*). These results indicate that Leu^{194} is a key amino acid for recruitment of TBK1.

TICAM-1 NTD Interacts with the TICAM-1-TIR Domain—We previously showed that recruitment of NAP1 and TBK1 to TICAM-1 requires homo-oligomerization through the TIR domain and the C terminus and RIP1 binding to the RHIM domain (15). Upon TLR3/4 ligand stimulation, homo-oligomerization is triggered by binding to dimerized TLR3 or TICAM-2, and overexpression of TICAM-1 induces homo-oligomerization (15). How TICAM-1 molecules are prevented from auto-activation in the resting state remains unresolved. TICAM-1 contains two structural domains, the NTD and the TIR domain, and Leu^{194} and the TRAF2/6-binding sites are between these domains. We hypothesized that these interacting sites are covered by the NTD to prevent downstream signaling molecules from accessing TICAM-1.

To test this hypothesis, we investigated the physical association of the NTD with truncated TICAM-1 fragments. FLAG-tagged NTD was coexpressed with HA-tagged TICAM-1-N, TICAM-1-TIR, or TICAM-1-C in HEK293FT cells, and coimmunoprecipitation was performed using anti-tag Abs. Notably, NTD coimmunoprecipitated with TICAM-1-TIR but

FIGURE 4. **Leu^{194} is indispensable for recruitment of TBK1 to TICAM-1.** *A*, confocal images show HeLa cells coexpressing HA-tagged wild-type (*WT*) TICAM-1 (*left panels*) or L194A mutant (*right panels*) and FLAG-tagged TRAF6, TRAF2, and TRAF3 or Myc-tagged NAP1. HeLa cells, transfected with the expression plasmids for HA-tagged wild-type TICAM-1 or L194A mutant (50 ng) and the indicated FLAG- or Myc-tagged signaling molecules (300 ng), were stained with anti-FLAG or anti-Myc mAb and anti-HA pAb, followed by Alexa Fluor 488-labeled goat anti-mouse Ab and Alexa Fluor 568-labeled goat anti-rabbit Ab. Colocalization of TICAM-1 with endogenous TBK1 was detected using anti-TBK1 pAb and Alexa Fluor 488-labeled goat anti-rabbit Ab. *Red*, wild-type and L194A mutant; *green*, TRAF6, TRAF2, TRAF3, NAP1, and TBK1; *blue*, DAPI-stained nuclei. *Bar*, 10 μm. *B*, recruitment of endogenous TBK1 to TICAM-1 by poly(I-C) stimulation. HeLa cells were transfected with the expression vector for HA-tagged wild-type TICAM-1 or L194A mutant (0.1 ng). Twenty four hours after transfection, cells were stimulated with buffer alone or 10 μg/ml poly(I-C) for 30 min. Fixed cells were labeled with anti-HA mAb and anti-TBK1 pAb, followed by Alexa Fluor 568-labeled goat anti-mouse IgG and Alexa Fluor 488-labeled goat anti-rabbit IgG. *C*, endogenous TBK1 physically associates with wild-type TICAM-1 but not the L194A mutant. *Left panels*, HEK293FT cells were transfected with empty vector or expression vectors for HA-tagged wild-type (*WT*) TICAM-1 or L194A mutant together with FLAG-tagged TRAF2, TRAF3. After 24 h, cells were lysed, and TICAM-1 was immunoprecipitated using an anti-HA pAb. *Right panels*, cells were transfected with empty vector or expression vector for HA-tagged wild-type TICAM-1 or L194A mutant. After 24 h, cells were lysed, and endogenous TBK1 was immunoprecipitated (*IP*) using an anti-TBK1 pAb. Rabbit IgG was used as a control Ab. The immunoprecipitants were resolved on SDS-PAGE (7.5% gel) under reducing conditions followed by immunoblotting (*IB*) with anti-tag mAb or anti-TBK1 pAb. Whole cell lysates (*WCL*) were subjected to immunoblotting with anti-FLAG mAb, anti-HA pAb, or anti-TBK1 pAb to detect protein expression (*IB*). Molecular weight markers are on the *right*.

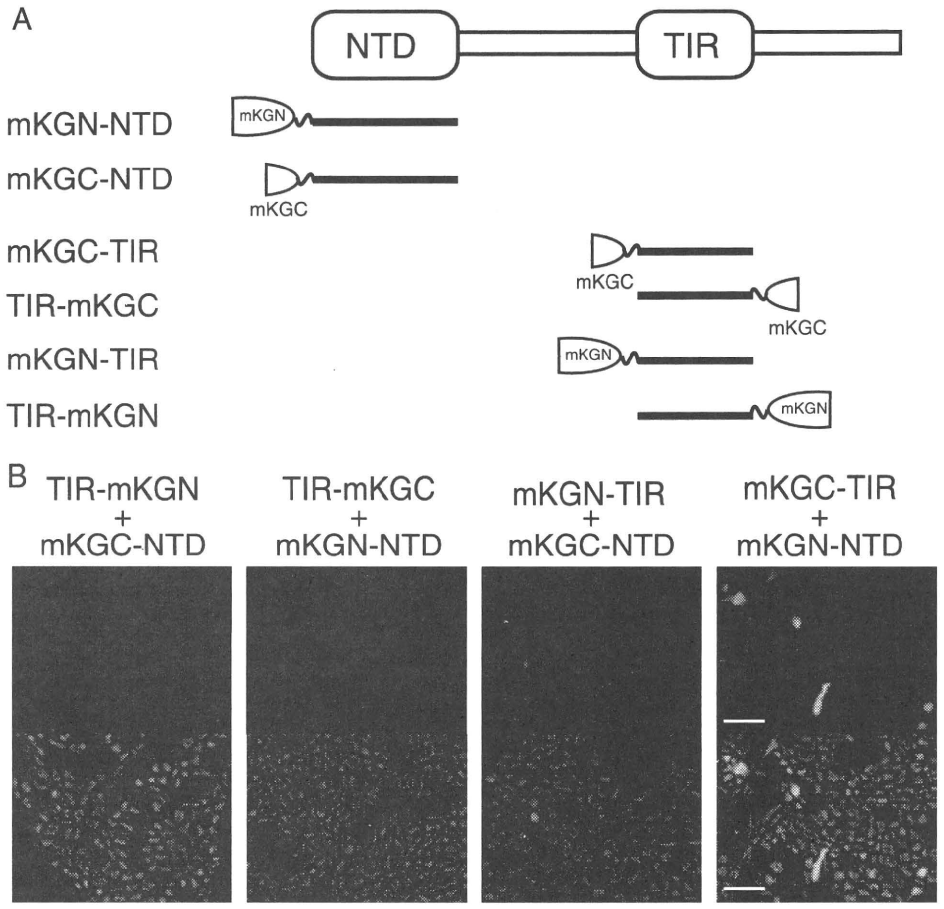

FIGURE 6. **NTD interacts with the N-terminal TICAM-1-TIR.** *A*, NTD or TICAM-1-TIR was fused to mKG fragments. *B*, fluorescence images show HEK293FT cells coexpressing NTD and TICAM-1-TIR, fused to mKG fragments at the N or C terminus. HEK293FT cells were transfected with the indicated combinations of expression plasmids for truncated TICAM-1 mutants fused to mKG fragments (each 500 ng). Twenty four hours after transfection, conditioned media were replaced with Dulbecco's PBS. Cells were visualized by fluorescence microscopy. Signal was detected in cells coexpressing mKGC-TIR and mKGN-NTD, and faint fluorescence was observed in cells coexpressing mKGN-TIR and mKGC-NTD. *Bar*, 100 μm.

not with TICAM-1-N or TICAM-1-C (Fig. 5), suggesting an intramolecular association between the NTD and the TIR domain. To further assess direct interaction between the NTD and the TIR domain, protein-protein interaction analysis was performed using a protein fragment complementation method. We made six constructs fusing the N- or C-terminal fragment of the monomeric Kusabira-Green protein to the N terminus of the NTD (mKGN-NTD, mKGC-NTD), the N terminus of the TIR domain (mKGN-TIR, mKGC-TIR), or the C terminus of the TIR domain (TIR-mKGN, TIR-mKGC) (Fig. 6*A*). Fluorescence was detected when expressed fused proteins interacted, restoring the mKG protein from the mKG fragments. HEK293FT cells were transfected with combinations of expression plasmids, and 24 h after transfection, strong fluorescent signals were detected in cells coexpressing mKGC-TIR and mKGN-NTD, and faint signals were detected in the cells coexpressing mKGN-TIR and mKGC-NTD (Fig. 6*B*). In contrast, cells coexpressing TIR-mKGN or TIR-mKGC and mKG-NTD did not fluoresce (Fig. 6*B*). These results strongly suggested that the NTD interacts with the N-terminal TICAM-1-TIR domain.

A TICAM-1 mutant lacking the NTD (Δ180) had high potential to activate the IFN-β promoter compared with wild-type TICAM-1 (Fig. 1*C*). This augmented activity of Δ180 mutant was more clearly shown when wild-type or Δ180 mutant was expressed at a low level (Fig. 7*A*). In HEK293 cells transfected with 0.1 ng of wild-type- or the L194A-expressing plasmid, wild-type TICAM-1 was inactive, whereas Δ180 mutant exerted the ability to activate the IFN-β promoter, although their protein expression levels were almost equivalent (Fig. 7*B*). Under these conditions, wild-type TICAM-1 diffusely localized in cytoplasm (Fig. 7*C*). In contrast, Δ180 mutant formed a speckle-like signalosome in unstimulated cells as seen in poly(I-C)-stimulated wild-type TICAM-1 (Fig. 7*C*), suggesting that deletion of the NTD facilitates the homo-oligomerization of Δ180 mutant through the TIR domain.

DISCUSSION

Activation of the transcription factor IRF-3 is a key downstream event in the signaling cascade of TICAM-1, resulting in induction of antiviral genes, including IFN-β. Direct binding of TICAM-1 to the IRF-3 activating kinase TBK1 is necessary for IRF-3 phosphorylation. Here, we identified Leu^{194} as essential in TICAM-1 for recruiting TBK1. Although Leu^{194} was critical for TBK1 binding, Ser^{189}, Arg^{195}, and Ser^{196} may stabilize the interaction.

TICAM-1 has two structural domains, the NTD and the TIR domain. Results from trypsin digestion of the TICAM-1 (1–566 aa) suggest the region between the NTD and the TIR domain forms a loose structure that might recruit downstream signaling molecules (24). Because the crucial amino acids for TRAF2, TRAF6, and TBK1 binding reside in this region, naive TICAM-1 may have a closed conformation that covers these sites. Indeed, using the protein-protein association analysis, we clearly showed that the NTD interacted with the N-terminal TIR domain. These observations suggest that the NTD folds into the TIR domain, preventing downstream signaling molecules from accessing their binding sites. Upon stimulation of TLR3/4, or TICAM-1 overexpression, TICAM-1 oligomerizes through the TIR domain and the C-terminal region (15). This may break the intramolecular association and induce a conformational change that allows downstream signaling molecules to their binding sites.

Deletion of the NTD augmented the TICAM-1 activity (Fig. 7). The association sites of TRAF2/6 and TBK1 are likely to be available in the Δ180 mutant. This would facilitate recruitment

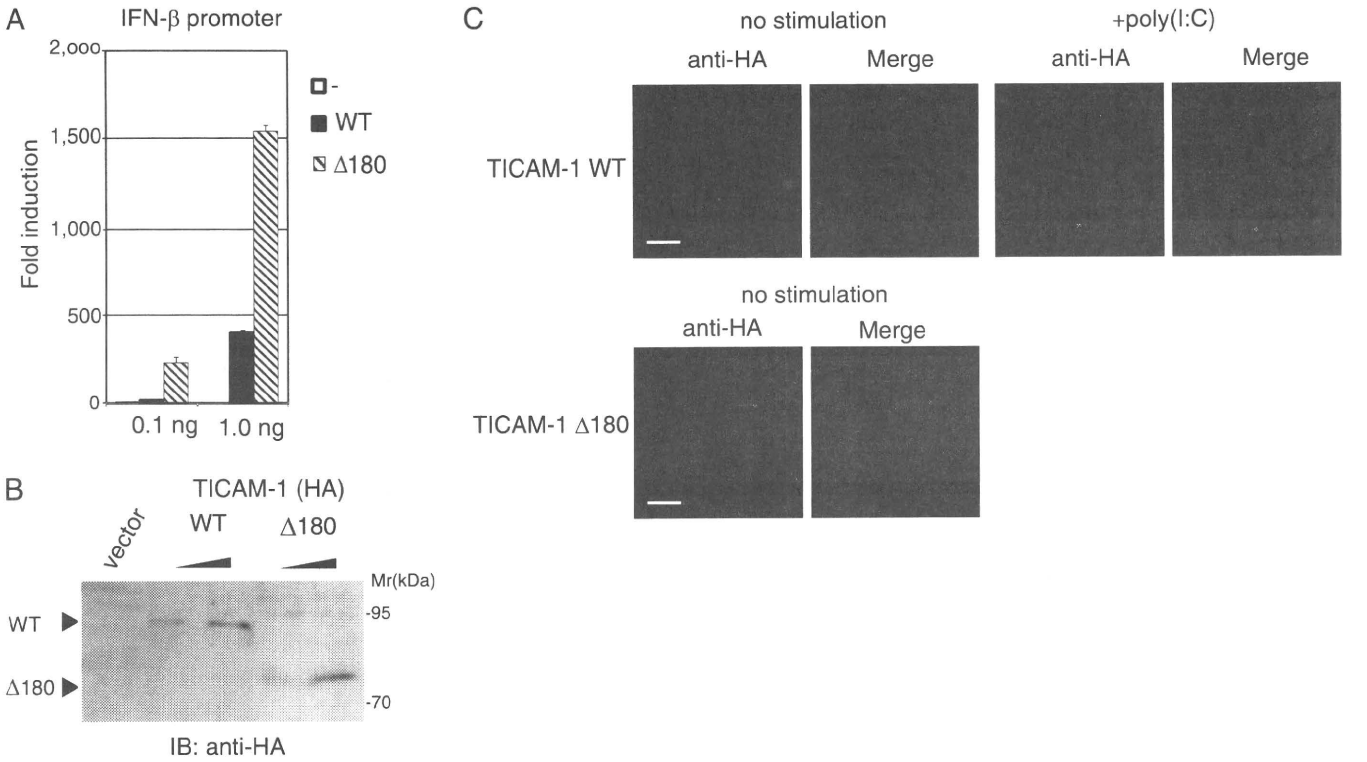

FIGURE 7. **Δ180 mutant had high potential to activate the IFN-β promoter compared with wild-type TICAM-1.** *A*, IFN-β promoter activation by the Δ180 mutant. HEK293 cells were transfected with empty vector or expression plasmid for wild-type (*WT*) TICAM-1 or Δ180 mutant (0.1 and 1.0 ng) together with the IFN-β promoter reporter. Luciferase activity was measured 24 h after transfection. Representative data from a minimum of four separate experiments, each performed in triplicate, are shown. *B*, protein expression of wild-type and the Δ180 mutant in HEK293 cell lysates. *IB*, immunoblot. *C*, confocal images of HeLa cells expressing a low level of HA-tagged wild-type TICAM-1 (*upper panels*) or Δ180 mutant (*lower panels*). Cells were transfected with the expression plasmid for wild-type TICAM-1 or Δ180 mutant (0.1 ng). After 24 h, cells were stimulated with buffer alone or 10 μg/ml poly(I-C) for 30 min, and fixed cells were labeled with anti-HA pAb and Alexa Fluor 568-labeled secondary Ab. The Δ180 mutant formed a speckle-like signalosome in unstimulated cells. *Red*, wild-type and Δ180 mutant; *blue*, DAPI-stained nuclei. *Bar*, 10 μm.

of the IRF-3 kinase complex. The Δ190 mutant showed reduced IFN-β promoter activation compared with the Δ180 mutant, probably because the absence of Ser^{189} stabilized TBK1 binding to TICAM-1 (Fig. 1*C*). Thus, the NTD may act as a repression domain within TICAM-1. Remarkably, exogenous NTD did not affect activation of IRF-3 or NF-κB by wild-type TICAM-1, the Δ180 mutant, or by TLR3-TICAM-1 activated with poly(I-C) (supplemental Fig. 1). We propose that exogenous NTD failed to interact with naive TICAM-1 because the TIR domain was occupied intramolecularly with NTD. Once TICAM-1 was recruited to TLR3, and oligomerized, the TRAF2/6 and TBK1 association sites appeared and signaling occurred quickly. When expressed with mutant Δ180, exogenous NTD interacted with the TIR domain of Δ180, whose binding site is distant from the TBK1 association sites, and did not affect TBK1 recruitment.

RIP1 binding to the C-terminal RHIM domain is necessary for TICAM-1 to mediate NF-κB activation (18), and the L194A mutant recruited RIP1 and activated NF-κB (Fig. 3*B* and supplemental Fig. 2). How NF-κB activation is controlled when TICAM-1 is in the resting form is unknown, but we surmise that the RHIM domain is unexposed in the resting state and that homodimerization opens the RHIM domain for RIP1 binding. Pro^{434} in the BB loop of the TICAM-1-TIR domain is critical for TICAM-1 homodimerization, but the C-terminal homodimerization determinant remains unidentified (15). Further analysis is required to elucidate the mechanism of TICAM-1 activation.

TICAM-1 acts as a platform that accumulates signaling molecules to the TICAM-1 signalosome and triggers diversified cellular responses. TICAM-1-dependent gene expression directs mDCs to activate natural killer cells and cytotoxic T lymphocytes, which are both the most effective for antiviral response, and are an anti-cancer immune response (8, 9). Indeed, TLR3/4 ligands are strong candidates for adjuvant anti-cancer and infectious disease immunotherapy (10, 27–29). Interestingly, the RIG-I-like receptor-mediated signaling pathway shares most of its downstream signaling molecules with the TICAM-1 pathway, but it plays a distinct role in antivirus immunity by producing type I IFNs (30). Although TICAM-1-mediated signaling is initiated from the endosome, RIG-I-like receptor-mediated signaling occurs at the mitochondrial outer membrane (31). Hence, compartmentalization of signal platforms might be significant for activating distinct transcription factors, resulting in different cellular responses.

In certain RNA viral infections, TLR3-TICAM-1-dependent inflammatory cytokine and chemokine production affects virally induced pathology and host survival (32). In addition, biased activation of the TLR4-TICAM-1 pathway in lung macrophages by oxidized phospholipids triggers acute lung injury through cytokine production (11). Therefore, control of TICAM-1 activation is a novel therapeutic target for acute lung

injury. The development of an inhibitory molecule that blocks homo-oligomerization of TICAM-1 might be a straightforward approach for controlling excessive activation of TICAM-1 after viral infection.

Acknowledgments—We are grateful to M. Sasai, K. Funami, A. Watanabe, H. Takaki, H. Shime, and T. Ebihara for invaluable discussions. Thanks are also due to T. Taniguchi (University of Tokyo) and M. Nakanishi (Nagoya City University, Nagoya, Japan) for providing the plasmids and to K. Arimoto (Kyoto University, Kyoto, Japan) and K. Shimotohno (Chiba Institute of Technology, Chiba, Japan) for providing reagents.

REFERENCES

1. Akira, S., Uematsu, S., and Takeuchi, O. (2006) *Cell* **124,** 783–801
2. Baccala, R., Hoebe, K., Kono, D. H., Beutler, B., and Theofilopoulos, A. N. (2007) *Nat. Med.* **13,** 543–551
3. O'Neill, L. A., and Bowie, A. G. (2007) *Nat. Rev. Immunol.* **7,** 353–364
4. Oshiumi, H., Matsumoto, M., Funami, K., Akazawa, T., and Seya, T. (2003) *Nat. Immunol.* **4,** 161–167
5. Yamamoto, M., Sato, S., Hemmi, H., Hoshino, K., Kaisho, T., Sanjo, H., Takeuchi, O., Sugiyama, M., Okabe, M., Takeda, K., and Akira, S. (2003) *Science* **301,** 640–643
6. Fitzgerald, K. A., Rowe, D. C., Barnes, B. J., Caffrey, D. R., Visintin, A., Latz, E., Monks, B., Pitha, P. M., and Golenbock, D. T. (2003) *J. Exp. Med.* **198,** 1043–1055
7. Oshiumi, H., Sasai, M., Shida, K., Fujita, T., Matsumoto, M., and Seya, T. (2003) *J. Biol. Chem.* **278,** 49751–49762
8. Schulz, O., Diebold, S. S., Chen, M., Näslund, T. I., Nolte, M. A., Alexopoulou, L., Azuma, Y. T., Flavell, R. A., Liljeström, P., Reis, e., and Sousa, C. R. (2005) *Nature* **433,** 887–892
9. Akazawa, T., Ebihara, T., Okuno, M., Okuda, Y., Shingai, M., Tsujimura, K., Takahashi, T., Ikawa, M., Okabe, M., Inoue, N., Okamoto-Tanaka, M., Ishizaki, H., Miyoshi, J., Matsumoto, M., and Seya, T. (2007) *Proc. Natl. Acad. Sci. U.S.A.* **104,** 252–257
10. Mata-Haro, V., Cekic, C., Martin, M., Chilton, P. M., Casella, C. R., and Mitchell, T. C. (2007) *Science* **316,** 1628–1632
11. Imai, Y., Kuba, K., Neely, G. G., Yaghubian-Malhami, R., Perkmann, T., van Loo, G., Ermolaeva, M., Veldhuizen, R., Leung, Y. H., Wang, H., Liu, H., Sun, Y., Pasparakis, M., Kopf, M., Mech, C., Bavari, S., Peiris, J. S., Slutsky, A. S., Akira, S., Hultqvist, M., Holmdahl, R., Nicholls, J., Jiang, C., Binder, C. J., and Penninger, J. M. (2008) *Cell* **133,** 235–249
12. Funami, K., Sasai, M., Ohba, Y., Oshiumi, H., Seya, T., and Matsumoto, M. (2007) *J. Immunol.* **179,** 6867–6872
13. Matsumoto, M., Funami, K., Tanabe, M., Oshiumi, H., Shingai, M., Seto, Y., Yamamoto, A., and Seya, T. (2003) *J. Immunol.* **171,** 3154–3162
14. Kagan, J. C., Su, T., Horng, T., Chow, A., Akira, S., and Medzhitov, R. (2008) *Nat. Immunol.* **9,** 361–368
15. Funami, K., Sasai, M., Oshiumi, H., Seya, T., and Matsumoto, M. (2008) *J. Biol. Chem.* **283,** 18283–18291
16. Sato, S., Sugiyama, M., Yamamoto, M., Watanabe, Y., Kawai, T., Takeda, K., and Akira, S. (2003) *J. Immunol.* **171,** 4304–4310
17. Fitzgerald, K. A., McWhirter, S. M., Faia, K. L., Rowe, D. C., Latz, E., Golenbock, D. T., Coyle, A. J., Liao, S. M., and Maniatis, T. (2003) *Nat. Immunol.* **4,** 491–496
18. Sharma, S., tenOever, B. R., Grandvaux, N., Zhou, G. P., Lin, R., and Hiscott, J. (2003) *Science* **300,** 1148–1151
19. Meylan, E., Burns, K., Hofmann, K., Blancheteau, V., Martinon, F., Kelliher, M., and Tschopp, J. (2004) *Nat. Immunol.* **5,** 503–507
20. Kaiser, W. J., and Offermann, M. K. (2005) *J. Immunol.* **174,** 4942–4952
21. Sasai, M., Oshiumi, H., Matsumoto, M., Inoue, N., Fujita, F., Nakanishi, M., and Seya, T. (2005) *J. Immunol.* **174,** 27–30
22. Häcker, H., Redecke, V., Blagoev, B., Kratchmarova, I., Hsu, L. C., Wang, G. G., Kamps, M. P., Raz, E., Wagner, H., Häcker, G., Mann, M., and Karin, M. (2006) *Nature* **439,** 204–207
23. Oganesyan, G., Saha, S. K., Guo, B., He, J. Q., Shahangian, A., Zarnegar, B., Perry, A., and Cheng, G. (2006) *Nature* **439,** 208–211
24. Horiuchi, M., Sakakibara, H., Kumeta, H., Takahashi, K., Enokizono, A., Ishii, A., Matsumoto, M., Seya, T., and Inagaki, F. (2008) *Biochem. Mol. Biol. Abstr.* **31,** 533
25. Honda, K., and Taniguchi, T. (2006) *Nat. Rev. Immunol.* **6,** 644–658
26. Sasai, M., Tatematsu, M., Oshiumi, H., Funami, K., Matsumoto, M., Hatakeyama, S., and Seya, T. (2010) *Mol. Immunol.* **47,** 1283–1291
27. Salem, M. L., Kadima, A. N., Cole, D. J., and Gillanders, W. E. (2005) *J. Immunother.* **28,** 220–228
28. Seya, T., and Matsumoto, M. (2009) *Cancer Immunol. Immunother.* **58,** 1175–1184
29. Longhi, M. P., Trumpfheller, C., Idoyaga, J., Caskey, M., Matos, I., Kluger, C., Salazar, A. M., Colonna, M., and Steinman, R. M. (2009) *J. Exp. Med.* **206,** 1589–1602
30. Yoneyama, M., and Fujita, T. (2009) *Immunol. Rev.* **227,** 54–65
31. Seth, R. B., Sun, L., Ea, C. K., and Chen, Z. J. (2005) *Cell* **122,** 669–682
32. Matsumoto, M., and Seya, T. (2008) *Adv. Drug Deliv. Rev.* **60,** 805–812
33. Funami, K., Matsumoto, M., Oshiumi, H., Akazawa, T., Yamamoto, A., and Seya, T. (2004) *Int. Immunol.* **16,** 1143–1154
34. Iwamura, T., Yoneyama, M., Yamaguchi, K., Suhara, W., Mori, W., Shiota, K., Okabe, Y., Namiki, H., and Fujita, T. (2001) *Genes Cells* **6,** 375–388

ELSEVIER

INSTITUT PASTEUR

Microbes and Infection xx (2011) 1–9

www.elsevier.com/locate/micinf

Original article

Failure of mycoplasma lipoprotein MALP-2 to induce NK cell activation through dendritic cell TLR2

Ryoko Sawahata [a,1], Hiroaki Shime [a,1], Sayuri Yamazaki [a], Norimitsu Inoue [b], Takashi Akazawa [b], Yukari Fujimoto [c], Koichi Fukase [c], Misako Matsumoto [a], Tsukasa Seya [a,*]

[a] *Department of Microbiology and Immunology, Graduate School of Medicine, Hokkaido University, N-15 W-7, Kita-ku, Sapporo 060-8638,Japan*
[b] *Department of Molecular Genetics, Osaka Medical Center for Cancer, Nakamichi 1-3-2, Higashinari-ku, Osaka 537-8511, Japan*
[c] *Department of Chemistry, Graduate School of Science, Osaka University, Toyonaka, Osaka 560-0043, Japan*

Received 1 September 2010; accepted 9 December 2010

Abstract

Macrophage-activating lipopeptide 2 (MALP-2), a mycoplasmal diacylated lipopeptide with palmitic acid moiety (Pam2), activates Toll-like receptor (TLR) 2 to induce inflammatory cytokines. TLR2 is known to mature myeloid dendritic cells (mDC) to drive mDC contact-mediated natural killer (NK) cell activation. Here we tested if MALP-2 activates NK cells through stimulation of TLR2 on mDC. Although synthetic MALP-2 with 6 or 14 amino acids (a.a.) stretch (designated as s and f) matured mDC to induce IL-6, IL-12p40 and TNF-α to a similar extent, they far less activated NK cells than Pam2CSK4, a positive control of 6 a.a.-containing diacyl lipopeptide. MALP-2s and f were TLR2/6 agonists and activate the MyD88 pathway similar to Pam2CSK4, but MALP-2s having the CGNNDE sequence acted on mDC TLR2 to barely induce external NK activation. Even the s form, with slightly high induction of IL-6 compared to the f form, barely induced *in vivo* growth retardation of NK-sensitive implant tumor. Pam2CSK4 and MALP-2 have the common lipid moiety but different peptides, which are crucial for NK cell activation. The results infer that MALP-2 is applicable to a cytokine inducer but not to an adjuvant for antitumor NK immunotherapy.

Keywords: Toll-like receptor 2; MyD88; Macrophage-activating lipopeptide 2; Dendritic cells; NK activation

1. Introduction

Macrophage-activating lipopeptide 2 (MALP-2) is a mycoplasmal diacylated lipopeptide with agonistic activity for Toll-like receptor (TLR) 2 [1]. Myeloid dendritic cells (mDC) and macrophages produce inflammatory cytokines in response to MALP-2 [1,2]. MALP-2 is proteolytically liberated from the parent lipoprotein of M161Ag [2,3] or MALP-404 [4], which is anchored on the outer membrane of *Mycoplasma fermentans*. Although the protease that specifically cleaves M161Ag into MALP-2 has not been identified, the peptide sequence of MALP-2 is determined by Mass spectrometry as S-[2,3-bis (palmitoyl)propyl]cysteine (Pam2Cys) followed by 14 amino acids [5] (Table 1). In fact, the TLR2 agonistic functions are conserved in a synthetic compound (herein referred to MALP-2f) [5]. This synthetic MALP-2 has been applied to clinical phase studies to develop a new adjuvant [6].

Several reports suggested that microbial pattern molecules have the ability to activate natural killer (NK) cells *in vitro* [7–10]. TLR and cytoplasmic pattern sensors are representative pattern-recognition receptors (PRR) which may be associated with mDC-mediated NK activation [7–9]. TLR3 and the adapter TICAM-1 (TRIF) in mDC typically participate in driving NK activation in response to dsRNA [10]. Recent studies on TLR2 agonists including lipopeptides also revealed that stimulation of TLR2 on mDC results in activation of the MyD88 pathway in mDC to drive external NK activation [11,12]. NK cells play a role in early defense against various pathogens.

* Corresponding author. Tel.: +81 11 706 5073; fax: +81 11 706 7866.
E-mail address: seya-tu@pop.med.hokudai.ac.jp (T. Seya).
[1] First two authors equally contributed to this work.

1286-4579/$ - see front matter © 2010 Institut Pasteur. Published by Elsevier Masson SAS. All rights reserved.
doi:10.1016/j.micinf.2010.12.003

Please cite this article in press as: R. Sawahata et al., Failure of mycoplasma lipoprotein MALP-2 to induce NK cell activation through dendritic cell TLR2, Microbes and Infection (2011), doi:10.1016/j.micinf.2010.12.003

Table 1
Lipopeptides used in this study.

Name	Peptide structure	Mr (Dalton)	Ref.
Pam2CSK	CSK	887.3	[19]
Pam2CSK4	CSKKKK	1271.8	[13]
Pam2Cys12	CSTSEVIGEKI	1716.2	[19]
MALP-2s	CGNNDE	1201.5	(*)[a]
MALP-2f	CGNNDESNISFKEK	2135.6	[13]

[a] * – This paper.

We have looked into the immuno-modulatory function of M161Ag and MALP-2, to develop a new adjuvant for cancer immunotherapy [1]. MALP-2 possessed high activity to induce IL-6, TNF-α, IL-10 and IL-12p40 from myeloid cells, but its functional potential for NK activation has not been examined yet. We test in the present studies whether MALP-2 has sufficient activity to induce NK cell activation *in vitro* and NK-mediated tumor regression *in vivo* using a mouse tumor implant model.

2. Materials and methods

2.1. Reagents and antibodies

The following materials were obtained as indicated: Fetal calf serum (FCS) from Bio Whittaker (Walkersville, MD), mouse granulocyte-macrophage colony-stimulating factor (GM-CSF) from PeproTech EC, Ltd (London, UK), the enzyme-linked immunosorbent assay (ELISA) kits for mouse (m)IFN-γ from Biolegend (San Diego, CA), IL-12p40 and IL-6 from eBioscience (San Diego, CA). Two forms of synthetic macrophage-activating lipopeptide 2 (MALP-2) were ordered to Biologica Co., Nagoya, Japan. MALP-2s: Pam2CGNNDE (MW; 1201.5) and MALP-2f: Pam2CGNNDESNISFKEK (MW; 2135.6). The synthesis of lipopeptides was achieved with a combination of solution- and solid-phase methods as described [13]. Pam2-Cys12 (Pam_2CSTSEVIGEKI), Pam2CSK4 (Pam_2CSKKKK) and control Pam2CSK were prepared as referenced [12]. PolyI:C, a TLR3 agonist for induction of antitumor immunity, was used for this study as a positive control.

The following antibodies were used: fluorescein isothiocyanate (FITC)-labeled anti-mouse CD69, I-Ab, IFN-ã mAb, phycoerythrin (PE)-labeled anti-mouse CD86, CD25, and allophycocyanin (APC)-labeled anti-mouse NK1.1 were purchased from Biolegend (San Diego, CA).

2.2. Mouse and cell lines

TLR2−/− and MyD88−/− mice were gifts from Dr. S. Akira (Osaka Univ., Osaka) as previously reported [14]. Female C57BL/6 mice were purchased from Clea Japan (Tokyo). Mice were maintained in our institute under specific pathogen-free conditions. All animal work was performed under guidelines established by the Hokkaido University Animal Care and Use Committee. Mice (12 weeks female C57BL/6) were housed four per cage and allowed food and water ad libitum. Animal studies were carefully performed without ethical problems.

HEK293 cells were obtained from ATCC and maintained in RPMI 1640/10% FCS. B16D8 cells were established in our laboratory as a subline of the B16 melanoma cell line [15] and cultured in RPMI 1640/10% FCS. This subline was characterized by its low MHC levels with no metastatic properties when injected s.c. into syngeneic C57BL/6 mice. The B16D8 cell line is a typical NK target [10].

2.3. Preparation of BMDC and spleen NK cells of mice

Mouse bone marrow-derived DC (BMDC) were prepared as described previously [16]. Spleen NK cells were positively isolated from spleens with DX5 Micro Beads kit (Miltenyi Biotech) [10]. The purity of NK cells ($DX5^+$ cells) was routinely about 80%. $DX5^+$ NK cells were used within 24 h.

2.4. Reporter assay

Plasmids (pEFBos) for expression of human TLR1, TLR2, TLR6 and TLR10 were prepared in our laboratory as described previously [16]. HEK293 cells were seeded onto 24-well plates and transfected with various amounts of expression vectors, the ELAM reporter gene, and the phRL-TK control plasmid using FuGene HD (Roche) according to the manufacturer's instructions. After 24 h, the cells were harvested in 50 μl lysis buffer. The luciferase activity was measured using Dual-Luciferase Reporter assay systems (Promega) and was shown as the mean ± S.D. of three experiments.

2.5. ELISA, flow cytometric (FACS) analysis of cell surface antigens

The levels of cytokines (IL-6, IL-12p40, IFN-γ etc.) were determined by sandwich ELISA (Amersham Pharmacia Biotech, Buckinghamshire, UK) or the message levels assessed by quantitative PCR [27]. Surface CD86 and I-Ab were determined by FACS using specific mAbs. The practical methods for FACS were described previously [16].

2.6. Assessment of in vitro cytolytic activity

The cytolytic activity of spleen NK cells was determined by ^{51}Cr assay as described previously [10]. NK cells were prepared from the spleen of C57BL/6 mice. NK cells were co-cultured with BMDCs at a ratio of 2:1 and 24 h later the mixtures were subdivided to assess NK-mediated cytotoxicity [10]. A B16 subline (D8) was used as a target cell. Target cells (2×10^3 cells/well) were coincubated with NK cells at the indicated lymphocyte to target (E/T) cell ratio (typically 15 and 30) in U-bottom 96-well plates in a total volume of 200 μl of RPMI 1640/10% FCS medium at 37 °C. Four hours later, the liberated ^{51}Cr in the medium was measured using the scintillation counter. Specific cytolytic activity was obtained by the formula: Specific cytotoxic activity (%) = [(experimental ^{51}Cr activity − spontaneous ^{51}Cr activity)/(total ^{51}Cr activity − spontaneous ^{51}Cr activity)] × 100. Each experiment was done in triplicate to confirm reproducibility of the results, and representative results are shown.

Please cite this article in press as: R. Sawahata et al., Failure of mycoplasma lipoprotein MALP-2 to induce NK cell activation through dendritic cell TLR2, Microbes and Infection (2011), doi:10.1016/j.micinf.2010.12.003

2.7. Tumor challenge and the treatment with Pam2Cys-containing peptides

B16D8 cells (6×10^5 cells) were subcutaneously (s.c.) transplanted into the back of mice at day 0. Pam2Cys-containing peptides (10 μg/head) or PBS (vehicle) only were injected around tumor at day 0, 3, 7, 9, 13, and 17. Tumor surfaces were measured twice a week by using a caliper.

3. Results

3.1. BMDC maturation and cytokine liberation in response to MALP-2

Pam2Cys-containing lipopeptides, Pam2Cys12, Pam2CSK, Pam2CSK4, and two forms of MALP-2 (s and f) were synthesized with reference to a previous report (Fig. S1) [13,17]. Pam2CSK was used as a negative control [17], which has virtually no cytokine-inducing activity (Fig. 1). By ELAM reporter assay, we assessed NF-κB activation potential of these lipopeptides (10–500 nM), and confirmed that all except Pam2CSK possess similar luciferin-activating potentials (data not shown).

IL-6 and IL-12p40 levels were determined by ELISA with the supernatant of the media where BMDC and each of the lipopeptides were co-cultured for 24 h. These cytokines were detected with high levels in the wells with Pam2Cys12, Pam2CSK4, MALP-2s and MALP-2f but not in Pam2CSK (Fig. 1A,B). These lipopeptides neither induced the mRNA of type I interferon (IFN), IL-15 and I-18 (data not shown) or produced less than the detection limit (<5 pg/ml) of IL-12p70 protein (Fig. 1C).

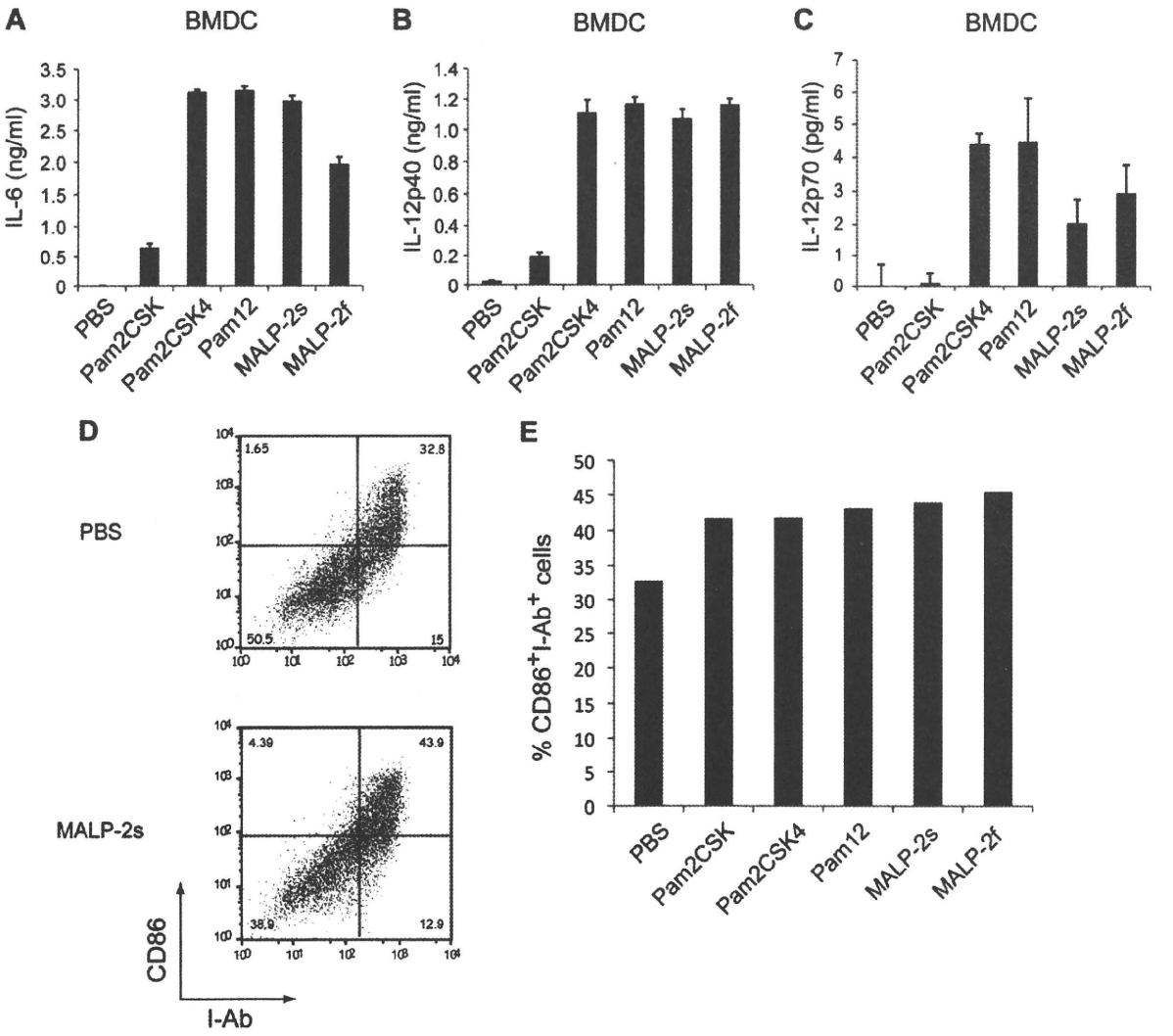

Fig. 1. BMDC cytokine production and maturation in response to TLR2 agonists (A, B, C) Cytokine production by BMDC stimulated with Pam2Cys-containing peptides. BMDC prepared from wild-type mice were treated with indicated Pam2Cys-containing peptides (100 nM) for 24 h. IL-6 (A), IL-12p40 (B), and IL-12p70 (C) concentrations in the supernatant were measured by ELISA. (D, E) Flow cytometric analysis of CD86 and I-Ab expression of BMDC stimulated with Pam2Cys-containing peptides. Typical examples of flow cytometric analysis (D). Summary of CD86 and I-Ab expression on the BMDC (E).

Please cite this article in press as: R. Sawahata et al., Failure of mycoplasma lipoprotein MALP-2 to induce NK cell activation through dendritic cell TLR2, Microbes and Infection (2011), doi:10.1016/j.micinf.2010.12.003